Bringing MEG towards clinical applications

Bushra Riaz Syeda

Department of Clinical Neurophysiology
Section of Clinical Neuroscience
Institute of Neuroscience and Physiology
Sahlgrenska Academy, University of Gothenburg,
Gothenburg, Sweden 2018

UNIVERSITY OF GOTHENBURG

Gothenburg 2018

Cover illustration: Spatial information density map indicating the regions of the right hemisphere to which a 7-channel on-scalp MEG system is sensitive.

Bringing MEG towards clinical applications

bushra.riaz@gu.se

ISBN 978-91-7833-103-1 (PRINT)
ISBN 978-91-7833-104-8 (PDF)

Printed in Gothenburg, Sweden 2018
Printed by BrandFactory

Dedicated to HOPE, of a new dawn.

Bringing MEG towards clinical applications

Bushra Riaz Syeda

Department of Clinical Neurophysiology, Section of Clinical Neuroscience,
Institute of Neuroscience and Physiology,
Sahlgrenska Academy, University of Gothenburg
Gothenburg, Sweden

ABSTRACT

Magnetoencephalography (MEG) is a passive, non-invasive functional neuroimaging technique for recording magnetic fields generated by neuronal currents in the brain. MEG provides a unique capability to map the electrophysiology of the brain with very high temporal resolution (below 1 ms) and fairly good spatial resolution (less than 1 cm). The advent of whole head MEG systems in the 1990s opened new perspectives in the understanding of the human brain. It has been used in the medical research setting for, among other things, understanding neurodegenerative diseases. However clinical applications of MEG are still few. One limiting factor is the sensors that are utilized in today's commercially available MEG systems: they operate only at extremely low temperatures. Liquid helium, an increasingly expensive and finite natural resource, is used to cool the sensors. Furthermore, thermal insulation that must be placed between the sensors and the subject limits system sensitivity. Modern sensor technologies operating at more moderate temperatures have led to developments towards principally new 'on-scalp' MEG systems. By eliminating the use of liquid helium and providing improved sensitivity via scanning closer to the brain, on-scalp MEG provides a promising future for MEG in clinical applications.

In this work, theoretical and experimental methods are detailed for on-scalp and conventional MEG studies of neural activations that are generally relevant to neuroscience research and clinical applications. As such, we bring MEG a step closer to becoming a routinely used clinical imaging modality.

The work is comprised of two main activities:

Activity I: Experimental support for utilizing MEG in a new clinical setting. We developed a MEG-based experimental approach for understanding the neural mechanisms and networks involved in modulating an individual's response to arousing stimuli. The aim is a non-invasive biomarker for identifying risk of developing cardiovascular disease. A MEG study was designed in line with previous microneurography studies that are known to reveal a distinct muscle sympathetic nerve activity (MSNA) response profile. This profile predicts the concomitant blood pressure trends associated with brief arousing stimuli and short periods of mental stress. In this thesis work, we investigated neural correlates of such MSNA response profiles in 20 subjects with MEG.

Activity II: Theoretical support for on-scalp MEG. We developed a framework for investigating realistic next generation MEG system designs. Our main metric is information capacity: a measure of the amount of information that can be extracted about brain activity with a given system. We use it to show the specific gains one can achieve by shifting to on-scalp MEG technology. This work furthermore contributed towards sensor array designs for full head MEG systems. The framework not only allows designing optimal arrays for MEG with new sensor technologies but also guides important sensor design parameters (such as pickup loop size, noise level, etc.) for on-scalp MEG systems.

In the future, these clinical and theoretical activities should be combined to develop a "custom on-scalp MEG" diagnostic procedure that includes improved sensitivity to cortical activations of clinical relevance.

Keywords: MEG, on-scalp, next generation MEG systems, high-T_c SQUIDs, arousal, muscle sympathetic nerve response.

ISBN 978-91-7833-103-1 (PRINT)
ISBN 978-91-7833-104-8 (PDF)

SAMMANFATTNING PÅ SVENSKA

Magnetencefalografi (MEG) är en passiv, icke-invasiv funktionell teknik för att avbilda de magnetfält som alstras av nervceller i hjärnan. MEG är unik i sin förmåga att kunna kartlägga elektrofysiologin i hjärnan med väldigt hög tidsupplösning (mindre än 1 ms) och ganska god rumsupplösning (mindre än 1 cm). MEG-system som täcker hela huvudet introducerades under 1990-talet. Detta öppnade upp nya perspektiv för förståelsen av den mänskliga hjärnans funktion och MEG har sedan dess använts i medicinsk forskning för att bl.a. förstå neurodegenerativa sjukdomar. De kliniska tillämpningarna för MEG är dock få. En begränsande faktor är att de sensorer som används i kommersiellt tillgängliga MEG-system kräver extremt låga temperaturer för att fungera. De kyls med hjälp av flytande helium, en allt dyrare och ändlig resurs. Dessutom krävs isolering mellan MEG-sensorerna och huvudet, vilket begränsar systemets prestanda. Modern sensorteknologi som fungerar vid högre temperaturer, har lett fram till nya så kallade ’on-scalp’-system. Genom att eliminera behovet av flytande helium och med placering av sensorer närmare hjärnan, vilket ger förbättrad sensitivitet, är ’on-scalp’-MEG en lovande utveckling för framtidens kliniska tillämpningar.

I det här arbetet beskrivs teoretiska och experimentella metoder för ’on-scalp’-, och konventionell MEG, vilka är relevanta för både neurovetenskaplig forskning och kliniska tillämpningar. Således för vi MEG ett steg närmare användning som rutinmässig klinisk undersökningsmodalitet.

Arbetet är uppdelat i två huvudsakliga spår:

Spår 1: Experimentellt stöd för att använda MEG för nya kliniska ändamål. Vi utvecklade ett MEG-baserat experimentellt tillvägagångssätt, för att förstå de centralnervösa mekanismer som är involverade i en individs respons till överraskningsstimuli (engelska: arousing stimuli). Målsättningen var att finna en neural, icke-invasiv, biomarkör för att identifiera risk för att utveckla hjärt- och kärlsjukdom. Vi designade en MEG-studie baserad på tidigare studier utförda med mikroneurografisk teknik, vilka har påvisat en distinkt reaktionsprofil i muskelbäddars sympatiska nervaktivitet (engelska: muscle sympathetic nerve activity, MSNA). Denna reaktionsprofil förutspår den medföljande blodtrycksförändringen som sker hos en individ i samband med överraskningsstimuli eller under kortvariga perioder av mental stress. I denna avhandling användes MEG för att undersöka den centralnervösa motsvarigheten till den perifera MSNA-svarsprofilen, hos 20 friska försökspersoner.

Spår 2: Teoretiskt stöd för ’on-scalp’-MEG. Vi utvecklade ett ramverk för hur man på ett realistiskt sätt kan utforska hur framtidens MEG-system bör konstrueras. Vårt främsta mått var informationskapacitet, dvs. den mängd information som ett givet (MEG-) system kan tillhandahålla om hjärnans aktivitet. Vi använde detta mått för att påvisa de specifika fördelarna som kan uppnås med ny ’on-scalp’-teknologi. Vårt arbete bidrar också till designen av nya sensoruppsättningar för MEG-system som täcker hela huvudet. Tillvägagångssättet som presenteras i denna avhandling ger möjlighet att inte bara optimera uppsättningar för MEG med ny sensorteknologi utan ger också vägledning i viktiga designparametrar för ’on-scalp’-system.

I framtiden bör de experimentella och teoretiska spåren i denna avhandling, kombineras för att utveckla skräddarsydd ’on-scalp’-MEG till ett redskap inom den kliniska diagnostiken.

LIST OF PAPERS

This thesis is based on the following studies, referred to in the text by their Roman numerals.

I. **B. Riaz**; J. J. Eskelin; L. Lundblad; B. G. Wallin; T. Karlsson; G. Starck; D. Lundqvist; R. Oostenveld; J. Schneiderman; M. Elam.

Cortical predictors for stress-induced cardiovascular disease.

Manuscript.

II. M. Xie; J. Schneiderman; M. Chukharkin; A. Kalabukhov; **B. Riaz**; D. Lundqvist; S. Whitmarsh; M. Hamalainen; V. Jousmaki; R. Oostenveld; D. Winkler.

Benchmarking for on-scalp MEG sensors.

IEEE Transactions on Biomedical Engineering 2016: **64**(6), pp. 1270-1276.

III. **B. Riaz**; C. Pfeiffer; J. Schneiderman

Evaluation of realistic layouts for next generation on-scalp MEG: spatial information density maps

Scientific Reports 2017: **7**(1), 6974.

CONTENT

ABBREVIATIONS

ACC	Anterior cingulate cortex
BEM	Boundary element model
EEG	Electroencephalography
ECoG	Electrocorticography
fMRI	Functional magnetic resonance imaging
HPI	Head position indicator
ICA	Independent component analysis
LCMV	Linearly constrained minimum variance
MEG	Magnetoencephalography
MNE	Minimum norm estimate
MRI	Magnetic resonance imaging
MSNA	Muscle sympathetic nerve activity
MSR	Magnetically shielded room
OPM	Optically pumped magnetometer
ROI	Region of interest
SID	Spatial information density
SNR	Signal-to-noise ratio
SQUID	Superconducting quantum interference device
SSS	Signal space separation
tSSS	Temporally-extended signal space separation

1 INTRODUCTION

Brain disorders cost the European Union ~800 billion euro in 2010 alone, thus constituting a major health economic challenge (Olesen et al., 2012). The burden furthermore goes well beyond economy: debilitating depression, severe dementia, psychotic episodes, etc. contribute to long periods of suffering for patients and those that care for them. Health-related issues aside, the human brain is the most complex and arguably most important organ in the body. For centuries scientists have been trying to understand the functionality of the brain. It is important to know, e.g., how the healthy brain works to keep it healthy and what exactly goes wrong when it is not. This has led to the development of many brain-imaging modalities capturing brain functionalities from different perspectives. Electroencephalography (EEG), for example, is one of the oldest and most commonly used techniques for recording brain activity. EEG measures the electrical activity of the neurons in the brain and as such gives a high temporal resolution. On the other hand, skin and skull impedances distort the recorded electrical signals, making localization of activity a challenge. Functional magnetic resonance imaging (fMRI) currently dominates the neuroimaging field because of its ability to deliver complete brain maps with isotropic resolution. However, as fMRI estimates neural activity indirectly by measuring modifications to cerebral blood oxygenation levels, it has inherently low temporal resolution. The best spatio-temporal resolution technique for investigating the human brain is presently electrocorticography (ECoG), or intracranial electroencephalography, where electrodes are directly placed on the cortex. However, as it is an invasive technique, it cannot be used on healthy subjects.

Magnetoencephalography (MEG) is a non-invasive method that records magnetic fields generated by electric currents from synchronously active neurons. Like EEG, MEG is a direct measure of neuronal activity and therefore has very high temporal resolution (less than 1 ms) and fairly good spatial resolution (less than 1 cm). The sources of EEG and MEG are the same - neuronal currents give rise to both electric and magnetic fields. However, unlike electric fields, magnetic fields are relatively unaffected by the tissues surrounding the cortex. Localizing neural activity with MEG is therefore more straightforward than with EEG. MEG has contributed significantly towards the understanding of brain functions ranging from sensory processing, motor actions and planning, cognition, language processing, social interaction, etc. (Hari and Salmelin, 2012). It has furthermore been used to produce promising results in diagnosis and understanding of neurodegenerative disorders like Parkinson's and Alzheimer's disease in the research set-

ting (Stoffers et al., 2008, Zamrini et al., 2011). However, established clinical applications are presently limited to epilepsy and presurgical mapping (Stufflebeam et al., 2009).

Commercial MEG systems are state-of-the-art in terms of functional neuroimaging spatiotemporal resolution; however, the low critical temperature Superconducting Quantum Interference device (low-T_c SQUID) sensors on which they are based, have not changed significantly since the 1990s. Low-T_c SQUIDs operate at T < 10 K which necessitates the use of liquid helium for cooling, thereby increasing the running cost of MEG systems. The liquid helium boil off, in a conventional MEG system, is roughly 100 liters per week. Moreover, around 2 cm of thermal insulation is required between the sensors and the room temperature environment in order to maintain the operating temperature of the low-T_c SQUIDs. This distance limits the sensitivity and spatial resolution of modern MEG systems.

MEG utilization, despite its remarkable spatiotemporal resolution, has not grown as rapidly as that of fMRI, even though both techniques were introduced in the same decade. fMRI benefited from existing MRI scanners that were modified for fMRI use, whereas MEG systems require not only sophisticated SQUID-based, helium-cooled sensor systems, but also a magnetically shielded room to acquire the data. Moreover, unlike fMRI, MEG presently requires more user intervention for reliable data analysis. Automated and user-friendly analysis could improve MEG utilization.

MEG being a sister modality to EEG, was initially thought to be redundant to EEG (Cohen et al., 1990) as the source of the signals in both are the same. However, the unique capability of MEG to resolve brain sources with good precision and thereby adding valuable information to brain imaging is now well established (Baillet, 2017). This is especially true for studies of networks, connectivity, and rapid communication within the brain. However, the complexity of data processing, maintenance and installation costs, and limited utilization areas are important issues that need to be treated for fully reaching MEG's potential in clinical applications.

The objective of this thesis project was to improve the clinical exploitation of MEG. The work is contributing in two main areas: first by exploring a new clinical application area that could benefit from MEG's unique capabilities, and second by paving a way towards next generation on-scalp MEG with new sensor technologies that would allow better spatial resolution with lower maintenance cost. Herein, I present the methods developed in these areas for

bringing MEG a step closer to clinical utilization. The specific aims of each part of the thesis contributing towards this main objective are as follows:

- To provide an overview and summary of MEG data collection and analysis procedures (Chapter 2). This part briefly presents the basic data acquisition and analysis routines in a MEG study. Readers familiar with MEG can skip this part.
- To demonstrate the clinical efficacy of a MEG experimental approach to investigate neural activations in relation to cardiovascular disease (Chapter 3).
- To summarize methods for evaluation and validation of next generation MEG sensor arrays. This can be utilized (a) for demonstrating the benefits of on-scalp MEG and (b) for designing next-generation on-scalp MEG systems (Chapters 4 and 5, respectively).

2 MAGNETOENCEPHALOGRAPHY

2.1. Sources of MEG signals

In MEG, the dominating source of the measured signal comes from the cerebral cortex. The cerebral cortex in humans is an approximately 2-4 mm thick layer of grey matter with at least 10^{10} neurons. It has a laminar structure with cell bodies of pyramidal neurons with parallel dendrites arranged in different layers. The dendrites of these neurons are aligned perpendicular to the cortical surface. MEG is mainly sensitive to cortical currents that are tangential to the skull, thus reflecting neuronal activity mainly from sulci of the cortex; the gyri of the cortex are less visible in MEG recordings. When a group of neurons in a cortical region are activated together, the postsynaptic currents in the dendrites of the neurons add together. The resulting signal can be approximated as an ideal current dipole. The ideal current dipole is a point source that has a direction, position, and magnitude, but no spatial extent. The magnetic field B at a location r of a dipolar point source with moment Q at location r_0 in a homogeneous volume is given by (Sarvas, 1987):

$$B(r) = \frac{\mu_0}{4\pi} Q \times \frac{r - r_0}{\left| r - r_0 \right|^3}$$

The magnetic field decreases rapidly as a function of the distance from the source. Thousands of neurons in the cortex activated at roughly the same time generate a magnetic field of 10-100 fT at the surface of the scalp, which is eight orders of magnitude smaller than the earth's magnetic field. To measure such a week signal, very sensitive sensors and a low-noise environment are required.

2.2. MEG sensors

The sensors conventionally used for measuring the weak magnetic fields from the brain are Superconducting QUantum Interference Devices (SQUIDs). SQUIDs require superconductivity, which is achieved by cooling the SQUID below a critical temperature (T_c) specific to the material of which they are composed. As such, these sensors require cryogenics to operate. SQUIDs are the most sensitive magnetic flux detectors and convert very small changes in magnetic flux to voltage. The magnetic flux is fed inductively to the SQUID through a flux transformer. Different flux transformers have different sensitivity profiles. The simplest design of flux transformers is the magnetometer in which a single superconducting loop picks up changes

in the enclosed magnetic field and couples it to the SQUID. Flux transformers with two coils, on the other hand, wound in opposing directions are called planar or axial gradiometers. The magnetic fields from distant sources are relatively uniform to both coils of a gradiometer (both axial and planar) with the resulting net flux to the SQUID equal to zero. Conversely, sources in closer proximity will generate differential flux in the coils, thereby generating a signal in the SQUID. Such transformers are relatively insensitive to background noise (see Figure 1). The sensitivity profile of an axial gradiometer is similar to a magnetometer whereas planar gradiometers are predominantly sensitive to sources located just beneath the loop.

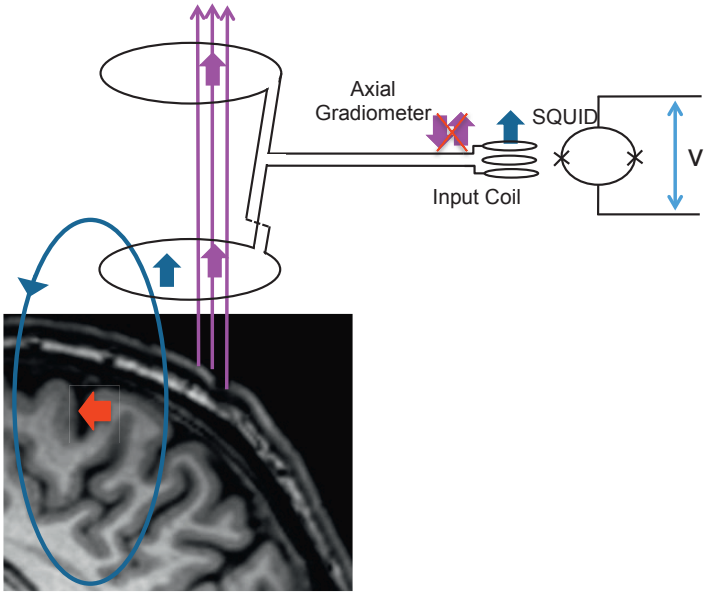

Figure 1. A magnetic field due to a small current in the cerebral cortex will cause current to flow in the superconducting coil of the flux transformer. In this case, the flux transformer is an axial gradiometer (i.e., with oppositely wound coils). The magnetic field drops sharply with distance; therefore the magnetic field (blue arrows) generated by the neural sources will couple more to the lower loop of the coil that is closer to the head. The background and more uniform environment noise (purple arrows) will couple equally to both loops of the coil, inducing equal and opposite current in two gradiometer loops. The flux transformer is connected to an input coil that is inductively coupling the flux to the SQUID. Only the magnetic flux (blue arrow) from the cortex will be coupled into the SQUID loop, the environment noise (purple arrows) will be cancelled out.

2.3. MEG measurements

State-of-the-art MEG systems consist of an array of a few hundred low-T_c SQUIDs (with either gradiometers or a combination of gradiometers and magnetometers) housed in a single helmet-shaped dewar and cooled with liquid helium to around T = 4.2 K. Such a dewar requires approximately 2 cm thick thermal insulation between the sensors and the outside, room temperature environment to maintain the low operating temperature for the SQUIDs.

The MEG measurement data used in this work was acquired at The Swedish National Facility for Magnetoencephalography (NatMEG), Karolinska Institutet, Stockholm, Sweden (www.natmeg.se). The MEG system deployed at NatMEG is an Elekta Neuromag® TRIUX system housed in Magnetically Shielded Room (MSR, model Ak3B, Vacuumschmelze GmbH). The Elekta system houses 306 SQUID channels (102 magnetometers and 204 planar gradiometers). They are arranged in 102 locations over the helmet with one magnetometer and two planar gradiometers overlapped at each location. MEG sensors are very sensitive to changes in magnetic flux; for reduction of external interference and background noise, MEG recordings are carried out in MSRs. The MSR at NatMEG has two layers of magnetic shielding along with external active shielding. The external active shielding provides extra protection for magnetometers from external environmental noise.

2.4. Source estimates from the recorded MEG signal

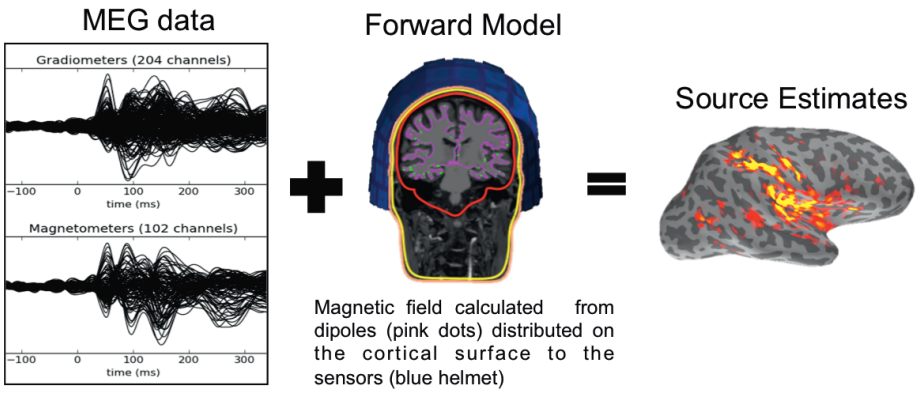

Figure 2. Estimation of source currents from acquired MEG data is performed via a solution to the so-called inverse problem. An inverse operator is calculated with a model of the forward solution, which is a calculation of the magnetic field at the sensors as generated by a predefined source distribution.

Estimating the location and time-course of brain activity from the measured MEG signal requires solving the so-called inverse problem (Figure 2). The inverse problem in MEG is ill posed; it does not have a unique solution because an infinite number of source combinations can theoretically generate the same data. However, including *a priori* information about the underlying neurophysiology allows for a unique solution. For example, source estimates can be restricted to the cortical mantle where they are modeled as current dipoles with a physiologically constrained density. The forward solution (also referred to as the gain matrix) is calculated by estimating the magnetic field from each dipole location to the sensors, taking into account the conductivity of the medium. For MEG, a single compartment Boundary Element Model (BEM, generated from a segmented MRI of the subject's head) is often used because (as mentioned previously) the magnetic field is only weakly affected by the tissues through which it passes. The inverse operator is estimated based on the gain matrix, sensor covariance, and making realistic assumptions on source covariance. The linear minimum norm estimates (MNE) inverse operator M can be calculated as (Hämäläinen, 2005).

$$M = R^{'}G^{T}(GR^{T}G^{T} + C)^{-1}$$

Where G is the gain matrix, C is the data/sensor noise-covariance matrix estimated from, e.g., an empty room recording (without the subject in the helmet) or pre-stimulus interval of the data. R is the source covariance. Different inverse operators have different assumptions/priors for estimation of R. The MNE selects the solution with the minimum L2 norm from all of the current distributions that can explain the data (Hämäläinen and Ilmoniemi, 1994).

The source amplitudes j at time t are estimated as follows:

$$j(t) = M \cdot x(t)$$

where x(t) is the recorded MEG data.

2.5. MEG study design

The first step in any MEG study is to define a research question and constraints of the measurement technique. MEG signals are mainly generated by the tangentially oriented cortical sources whereas radially oriented sources are better detected with EEG. The magnetic field furthermore decreases as a function of distance; therefore, deep sources are less visible with MEG and thus require more averages for the same signal-to-noise ratio (SNR). The study question is thus best defined keeping such constraints in mind. Once

the study question is defined, the next step is to design a MEG protocol to evoke the desired response so that, e.g., activated brain regions can be studied. The stimulus type, strength, duration, and inter-stimulus intervals must also be designed according to the research question. The number of stimulus repetitions, i.e., trials, required to estimate the source activity depends upon the expected SNR of the desired response. For example, the so-called N20 response in somatosensory evoked fields is around 100 fT in magnitude: such strong signal-levels can be observed at the single-trial level with magnetometers whose noise levels are below ~10 fT/√Hz. Performing pilot experiments with subsequent optimization of the study protocol is a sound approach to test the feasibility and validity of the study.

2.6. Data acquisition

The whole process of data acquisition, including checklists for subject preparation, and MEG system preparation, and log sheet for the recordings for the Arousal study, is included herein as Appendix for reference points.

2.7. Data analysis

The basic steps/pipeline for analyzing MEG data acquired from the Elekta Neuromag® system we use, is summarized in the flowchart shown in Figure 3. The analysis is carried out in Python and MATLAB, using custom code and the open source software packages MNE (Gramfort et al., 2013, Gramfort et al., 2014) and FieldTrip (Oostenveld et al., 2011). The MNE- and Fieldtrip toolboxes provide built-in functions for filtering, averaging, forward and inverse calculations, plotting and graphical user interfaces (GUIs) for visualizing MEG data and source estimates at the cortical level.

Maxfiltering and movement compensation

The data we acquire from the Elekta Neuromag® system is with active shielding on. The active shielding compensates noise by locally generating a field to oppose the noise. The data acquired is then filtered with the Maxfilter™ software (Elekta Oy, Finland). Maxfiltering compensates for artifacts of active shielding, and also provides additional features like head movement correction and artifact removal of external noise by Signal Space Separation (SSS) and temporally-extended SSS (tSSS) methods (more details on these below). During MEG recordings, the position of the subject's head relative to the MEG sensor array can be continuously tracked using head position indicator (HPI) coils that are attached to the subject's head. The HPI coils are powered with different frequencies. This allows extracting the field strength of each HPI coil separately from the measured data, based on which the posi-

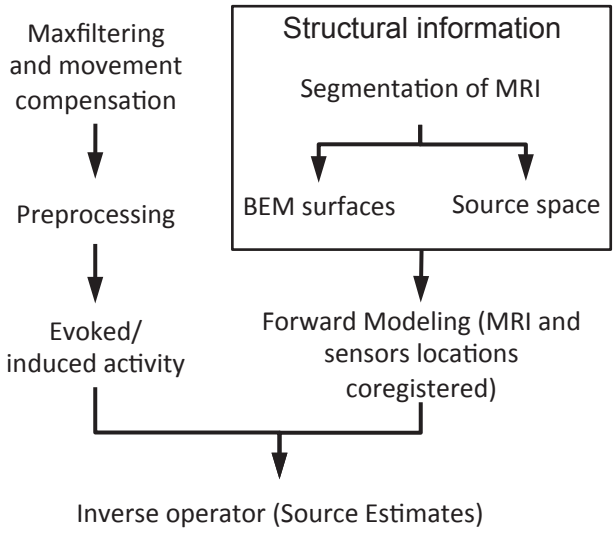

Figure 3. Flow chart summarizing the processing steps of MEG data

tion of the head inside the helmet can be estimated. These continuous head movement positions are used in conjunction with SSS or tSSS for continuous head movement compensation implemented in the Maxfilter software. The algorithm is based on transforming the measured signals into virtual channels/signal space calculated through SSS or tSSS in a device-independent representation in the head coordinate system. Virtual signals at the sensor locations are then calculated from the initial head position of the recording.

SSS is a mathematical method for removal of external interference and sensor artifacts (Taulu and Simola, 2006). It is a spatial filtering method based on the concept that the signal space can be divided into two subspaces/bases: an inner source signal subspace (sources within the sensor array) and an outer noise subspace (sources outside the sensor array). SSS removes artifacts by rejecting the noise subspace and thereby reconstructs a cleaner signal that is more dominated by the inner source space. tSSS is a temporal extension of SSS (Taulu and Hari, 2009). Like SSS, tSSS removes noise and artifacts but it is also able to remove artifacts with a spatially complex subspace that overlaps both inner signal subspace and outer noise subspace (like artifacts from braces, pacemakers, etc.). The signals that are temporally correlated in both subspaces are removed from the data and are considered artifacts because the brain signal represented by the inner subspace should not leak into the outer

noise subspace. In the case of no temporally correlated components, tSSS gives similar results as SSS.

The MEG data in this work has been filtered using tSSS using head movement compensation.

Preprocessing

This step includes filtering, and removal of artifacts. The data is filtered according to the frequency range of the expected activity. The next step is to remove 'physiological' artifacts, caused by eye movements and heartbeats, from the data. One of the commonly used methods for artifact rejection is Independent Component Analysis (Hyvärinen and Oja, 2000). ICA decomposes the data into statistically independent components (ICs). ICs are then correlated with the Electrooculogram (EOG) and Electrocardiogram (ECG) that have been sampled alongside the MEG recording. ICs that are correlated with the EOG and ECG, respectively, are removed and the 'cleaned' MEG data is subsequently reconstructed from the remaining ICs. A sample time course and topographical map of ICs representing cardiac and ocular artifacts for one of our subjects are shown in Figure 4.

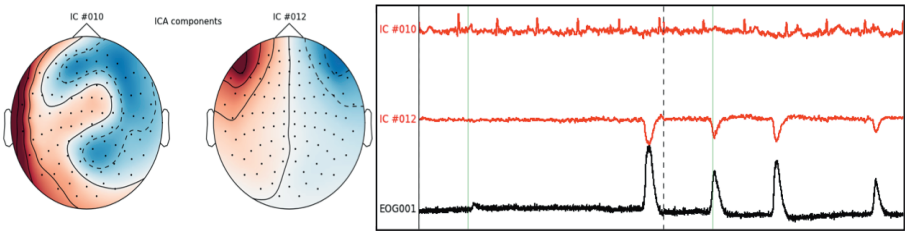

Figure 4. Automatically generated topographical map of the cardiac (left) and ocular (middle) artifacts along with the time course of the ICs in the right panel. The top time course is for 10 seconds of data segmented in two 5-sec epochs. Time courses for ICs are marked red for the cardiac (top) and ocular (middle). The black trace is from the horizontal EOG channels.

Averaging time- and frequency-domain activity

After artifact removal, the data is cropped around the stimulus into epochs. The time-domain activity in response to the stimuli is analyzed by averaging the epochs. Sample butterfly plots, where data from all the sensors has been time-locked and collapsed onto the same axis, and topographical plots for averaged/evoked somatosensory stimuli (electrical stimulations to the finger) are shown in Figure 5.

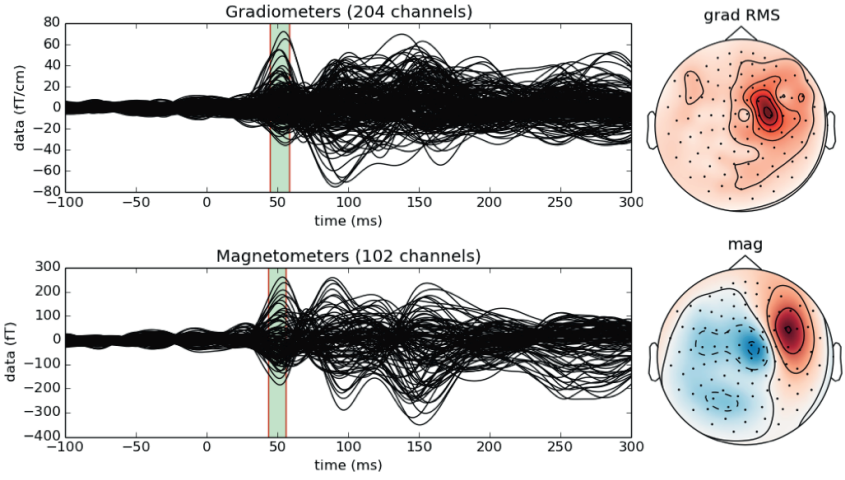

Figure 5. Left panels: butterfly plots of evoked data with gradiometer (top) and magnetometer channels (bottom). The highlighted time-window (green) in the butterfly plots is averaged and plotted in the two topographical maps on the right.

The frequency-domain activity, i.e., neural oscillations in response to stimuli (such as the reduction in amplitude of alpha-band signals between 8 and 12 Hz after presentation of some stimulus), is studied by spectrally decomposing the epochs followed by averaging (also known as time-frequency analysis).

These time- and frequency-domain responses can subsequently be localized to the cortical level as source estimates using the inverse operator of choice (for example, MNE, sLoreta, etc).

Structural information for MEG data

Structural information is added to the MEG data from a brain MRI of the subject. The T1-weighted MRIs are segmented using an automated pipeline in the FreeSurfer software package (Dale et al., 1999, Fischl et al., 1999). The surface midway between white and grey matter is used for setting up the source space. A grid of dipoles with appropriate spacing is arranged on that surface. A FreeSurfer-based watershed algorithm is furthermore used to generate the triangulations of the inner skull, skull, and scalp surfaces.

Forward calculation

The magnetic field at the sensor locations due to a dipole source on the cortical surface, i.e., the forward solution, is calculated using a BEM. As magnetic fields are only weakly affected by the different conductivities of the mediums, a single compartment BEM (inner skull), assuming the shape of the

intracranial volume, provides a reasonable solution. However, when MEG and EEG data are analyzed together, a three compartment BEM (inner skull, skull, and scalp) is required.

Calculation of the forward solution (a.k.a. the Gain or lead field matrix) requires co-registering of the anatomical MRI with the sensor locations. This is performed by aligning the set of fiducials (usually nasion and pre-auricular points) and head points acquired in the digitization process with the scalp surface from the MRI of the subject.

Inverse operator/ Source estimates

The inverse operator is calculated for estimating the sources generating the evoked and/or induced response at the cortical (source) level. The data covariance is estimated based on a pre-stimulus interval or empty room recording (without the subject in the MEG helmet). The source covariance is selected according to the chosen inverse method. The source estimates can then be calculated and visualized on the cortical surface.

3 AROUSAL

Hypertension is the most important of cardiovascular risk factors, entailing a major share of the global disease burden (Forouzanfar et al., 2015). If risk for hypertension could be established, then targeted treatments could relieve this burden. However, decades of research have yet to establish a reliable and clinically-accessible predictor for hypertension development. As such, should MEG be capable of identifying such a risk measure, the clinical utilization of MEG would expand significantly. In this section we investigate cortical biomarkers for predicting risk of cardiovascular disease. The objective was to identify clinically relevant and non-invasive correlates for what is today an established predictor for hypertension: muscle sympathetic nerve response to arousal. Previous studies on healthy males have shown that the invasive and extremely delicate measurement of an individual's muscle sympathetic nerve activity (MSNA) response to arousal is strongly correlated with the blood pressure response to stress (Donadio et al., 2012). As such, the muscle sympathetic nerve response can serve as a potential biomarker for assessing risk for hypertension and cardiovascular diseases. Studies with fMRI furthermore implicate specific brain regions as part of the central autonomic network that modulates sympathetic control. However, because the muscle sympathetic arousal response occurs rapidly (within a heartbeat or two at most), the limited time resolution inherent to fMRI makes it impossible to follow the communication between the responsible brain regions with this method. EEG provides a high temporal resolution; however, for our purposes, source localization is paramount. MEG is therefore a natural choice for elucidating the neural response to stress and identifying a non-invasive biomarker for risk of cardiovascular disease.

3.1. INTRODUCTION

The following introduction is meant to provide a thorough understanding of our study motivation, based on previous studies/results related to muscle sympathetic nerve activity (MSNA). Focus is placed on those parts that have guided the design of our MEG study (e.g., the timing of stimulus presentation) and the analysis pipeline (e.g., identifying regions of interest). Emphasis is furthermore placed on the goal of achieving clinically relevant results.

The fight-or-flight response, also known as the hyper arousal or acute stress response, is a physiological reaction in which the body prepares to deal with stress. This transitory reaction includes an elevation of blood pressure, tachycardia, and an increase in blood flow to skeletal muscles by inhibiting the vasoconstrictor activity in muscle sympathetic nerves. Microneurography studies on healthy subjects showed that an MSNA inhibitory response, similar to that of the fight-or-flight response, was observed when startling/arousing stimuli (visual flash, auditory beep or electrical stimulation to the finger) were delivered to subjects in sync with the baroreceptor afferent volley to the brain (200 ms after the R-wave of the ECG) (Donadio et al., 2002a, Donadio et al., 2002b, Eder et al., 2009). However, this response profile showed significant inter-individual differences. In ~50% of subjects, the startling stimuli evoked short-lasting inhibition of MSNA and less stimulus-induced increase in blood pressure, as compared to the other ~50% of subjects that showed weaker or no inhibition—and sometimes amplification—of MSNA (Donadio et al., 2002a, Donadio et al., 2002b). Further studies demonstrated that this MSNA response profile in relation to arousing stimuli is linked to cardiovascular responses during stress. Subjects that tend to inhibit MSNA bursts (hereon referred to as Inhibitors) have a weaker blood pressure increase when subjected to mental stress. Non-Inhibitors (with no effect or increased MSNA following an arousing stimulus), on the other hand, exhibited higher and sustained blood pressure increases when subjected to mental stress (Donadio et al., 2012). This MSNA inhibition response profile was furthermore reproducible over 6 months suggesting that response behavior is a characteristic for the individual and defines how they react to arousing stimuli (Donadio et al., 2002b). The specific profile of an individual, i.e., being an Inhibitor or a non-Inhibitor to stress/startling stimuli, presumably gives an insight into how individuals cope with environmental stress. Given that environmental stress and the development of high blood pressure and cardiovascular mortality are closely related (Timio et al., 1988, Timio et al., 1997), higher and sustained blood pressure response in non-Inhibitors to arousing or stressing stimuli increases their risk of developing

cardiovascular disease. As such, identifying a non-invasive biomarker for the MSNA inhibition response and developing therapies to modify it may decrease individuals' risk for developing cardiovascular disease.

The sympathetic nervous system (SNS) primarily orchestrates the body's fight-or-flight response and also contributes to maintaining homeostasis. MSNA, a subdivision of the SNS, is composed of vasoconstrictor pulses grouped in bursts that are regulated by baroreflexes. MSNA bursts usually occur in synchrony with the cardiac cycle and are involved in cardiovascular homeostasis (Wallin et al., 1975, Wallin and Fagius, 1988). The central autonomic control of this cardiovascular response pattern (necessary for homeostasis) is modulated by the central autonomic network. Such control includes feedback from cortical and subcortical brain regions (Damasio et al., Benarroch, 1993). Experimental human studies have contributed to identifying components of this network (Critchley et al., 2000, Gianaros et al., 2004); however, there is only limited understanding of how these cortical and subcortical brain areas modulate peripheral autonomic control in humans. The set of discrete cortical and subcortical brain areas repeatedly reported in the literature to be part of this central autonomic network and cardiovascular control in humans includes the anterior cingulate cortex (ACC) (Pool and Ransohoff, 1949, Critchley et al., 2003, Vogt and Derbyshire, 2009), insular cortex (Oppenheimer et al., 1991, Oppenheimer et al., 1992, Craig, 2002) and amygdala (Bechara et al., 1995, Critchley et al., 2000, Asahina et al., 2003).

In addition to studying human brain regions involved in regulating changes in autonomic activity, many studies have also investigated the influence of specific phases of the cardiac cycle on central processing of external stimuli (visual detection, perceived pain, or reflexive responses) (Edwards et al., 2002, Edwards et al., 2008, Park et al., 2014). For example, somatosensory input at different phases of the cardiac cycle has been shown to activate differential brain activity in an fMRI study (Gray et al., 2009). While it is unclear whether the arousal reaction itself is influenced by specific phases of the cardiac cycle, the arterial baroreflex modulation of MSNA is quite pronounced (Delius et al., 1972). In microneurography studies arousal stimuli elicited the strongest transitory changes in MSNA when they were synced with the baroreceptor afferent volley, roughly 200 ms after the R wave of the ECG. Inhibition was not significant when the stimulus coincided with the ECG R wave or was delayed by 600 ms (Macefield et al., 1998).

The objective of this study was to investigate the brain regions and underlying neural mechanisms responsible for, or correlated with, MSNA response

profiles (that have been characterized, and were heretofore only observable, with microneurography). In this study, the MEG protocol is designed such that it closely follows the microneurography arousal test, which is known to elicit clear transitory changes in the MSNA response. A pilot run with two subjects (one Inhibitor and one non-Inhibitor) indicated differences in beta frequency responses. Therefore, we focused our analysis on oscillatory responses in only three cortical brain regions, two of which are implicated to be part of central autonomic network: ACC and insular cortex. We also investigated the response of the Rolandic area (as we utilize somatosensory stimuli). We hypothesized that neural responses accompanying MSNA regulation might be revealed in these brain areas.

3.2. METHODS

3.2.1 Study design

In several previous microneurography studies, the arousing stimulus consisted of an electrical pulse to the index finger triggered with a delay of 200 ms after the ECG R-wave. A set of 36 such electrical pulses interspersed with 36 dummy stimuli (triggering pulse, but no electrical stimulation) were applied to the subjects with an inter-stimulus interval (ISI) of 30 to 60 s. The dummy pulses were used to contrast the standard heartbeat cycle related MSNA changes with that which was induced by stimuli.

In our initial attempt in translating this protocol to MEG, the dummy stimuli were replaced by electrical pulses to the index finger triggered with the ECG R-wave without a delay. The rationale behind this choice was based on the idea that the inhibition of MSNA activity is negligible when the arousing stimuli coincide with the ECG R-wave peak. A significant challenge in the analysis of this MEG protocol was the fact that the cardiac artifact was prominent in the averaged response when the stimuli were time locked with the ECG. Advanced signal processing techniques like ICA reduced the artifact, but were not able to completely remove it. The comparison of these two stimulus conditions was therefore unreliable.

An alternative study design was implemented that included a series of 5 electrical pulses. Each of these pulses was triggered with a delay of 200 ms on 5 consecutive ECG R–waves, in line with an earlier microneurography study (Donadio et al., 2002a, Donadio et al., 2002b). Donadio demonstrated that the arousal response from the 5th pulse was negligible as compared to the 1st, and indicated that habituation is likely the cause. This protocol is attractive for our MEG study because we can compare/contrast the responses to the 1st and 5th pulses, while potentially revealing temporal dynamics of habituation in between. However, the pilot run from this protocol showed that the brain response from, e.g., the first pulse had not returned to baseline before the arrival of the second one. In this case, the ~700 ms interval between two consecutive pulses (depending on the heart rate of the subject) was deemed to be too short. In order to have a sufficiently long time-window for the brain to return to some level of baseline in order to analyze the dynamics of the response to each pulse, the protocol was modified as follows: 3 pulses were triggered with every other heartbeat instead of consecutive heartbeats (i.e., the 2nd and 4th pulses were eliminated from the previous 5-pulse sequence) as shown in Figure 6.

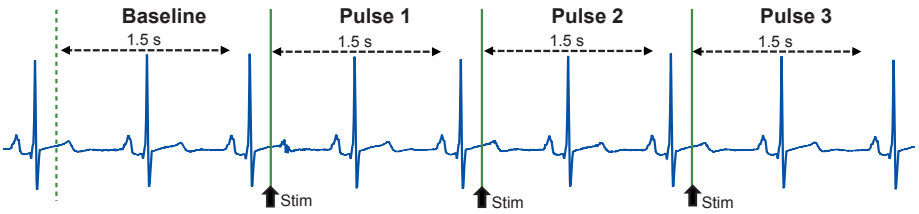

Figure 6. MEG study design showing electric stimulation events with respect to the heartbeat. The vertical green lines indicate the application of electric stimulation, delayed 200 ms after the R-wave (highest peak) of the electrocardiogram (blue trace). The green dotted line indicates the start of the baseline interval used in the analysis. A 1.5 s interval (black dashed lines) after each stimulation was used in the time frequency analysis.

The number of pulse train repetitions is 72, amounting to around 70 mins of recording time in line with the previous microneurography study. MEG recordings could benefit from increasing the number of repetitions: doubling the recording time boosts the power-SNR by 1.4 times. However, subjects tend to lose focus if the recording sessions are too long.

3.2.2 Preprocessing

The data acquired was filtered in the 0.5-40 Hz frequency range. The epochs were manually inspected for artifacts. Epochs with bad data segments, i.e., SQUID noise, movement artifacts, etc., were rejected from further analysis. ICA was used to reduce ocular and cardiac artifacts. We rejected 2-4 ICs for each subject. The detailed preprocessing steps are provided in the Methods section of Paper I.

3.2.3 Source estimates

To investigate the oscillatory response in selected regions of interest (ACC, insular cortex, and Rolandic area, including precentral and postcentral sulci), we used the linearly constrained minimum variance (LCMV) beamformer spatial filtering method. This source reconstruction approach is recommended for localizing oscillatory responses (Hansen et al., 2010). Instead of morphing to a common brain, the spatial filters were calculated for volumetric labels of the selected ROIs based on each individual's MRI FreeSurfer segmentation. Anatomical labels were then shrunk into functional labels covering only the activated vertices (60% of the peak response was selected as a threshold) in the label. A single trial-to-trial time series was extracted for each functional label at each region of interest. The time series was spectrally decomposed in the 5-40 Hz frequency range and averaged. The spectral pow-

er in all three pulses was normalized to the pre-stimulus interval that preceded the 1st pulse. More details regarding the MEG source analysis is covered in the Methods section of Paper I.

3.2.4 Statistics

We used a non-parametric, cluster-based permutation test (Maris and Oostenveld, 2007) to investigate whether the spectral response was significantly correlated with MSNA inhibition ($p<0.05$, two-sided, 1 000 permutations). This statistical test provides a straightforward approach for resolving the multiple comparison problem that can otherwise plague MEG and EEG data analysis because of the large number of sensors/sources and time points to be analyzed. The clusters of time-frequency points with above threshold correlations between spectral power and MSNA response were identified for each ROI and all three pulses. We used the Spearman coefficient for calculating all correlations.

3.2.5 Exploratory analysis

Apart from the analysis reported in Paper I, we investigated evoked responses and connectivity between selected ROIs as is discussed below. With the limited number of subjects in the study, this analysis was exploratory in nature and preliminary findings can thus be used for future studies. We also analyzed responses in other brain regions that might be involved in the processing of the arousal response.

Evoked responses

We used two source estimate methods: LCMV and minimum norm estimates (MNE), and explored evoked responses in the selected ROIs with both. The evoked responses with LCMV source estimates did not show a significant correlation with MSNA for any of the three pulses. For MNE-based current estimates, the evoked responses were noise normalized by dividing the current estimates with the variance, as explained (Dale et al., 2000) that resulted in dimensionless statistical variable known as dynamic statistical parameter maps (dSPM). The dSPM-evoked responses were compared between Inhibitors and non-Inhibitors on a group level, rather than correlating the responses with MSNA. We investigated the evoked responses to Pulse 1, Pulse 3, and the difference between Pulses 3 and 1 in all three ROIs. The difference of Pulses 3 and 1 was investigated to highlight arousal effects, as Pulse 1 is arousing whereas Pulse 3 is expected. We found differences on a group level in the insular cortex (both hemispheres) for the evoked response to Pulse 3 (shown in Figure 7); however, the differences were only marginally significant (right hemisphere $p=0.07$, left hemisphere $p=0.05$). These p values were

corrected for multiple time instances that were investigated through non-parametric cluster-based statistics; they were not, however multiple-comparison corrected for ROIs. No significant differences were found in response to Pulse 1 or in the difference in the response between Pulses 3 and 1 in the selected ROIs.

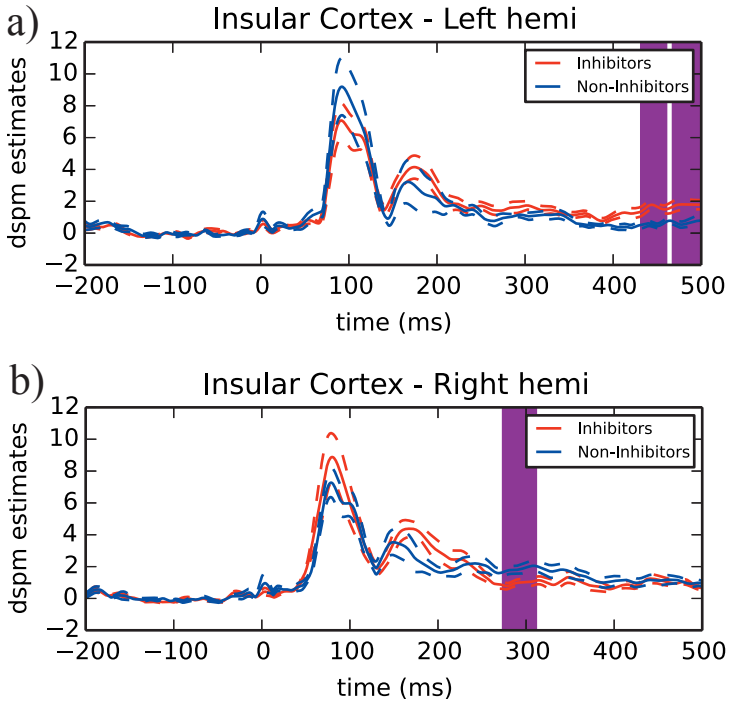

Figure 7. Evoked responses for Inhibitors (N=9, red) and non-Inhibitors (N=9, blue) extracted from the insular cortex functional label in the left and right hemispheres. The dashed blue and red lines indicate standard error of mean. The purple highlighted area shows the time points with significant ($p<0.08$) group differences between Inhibitors and non-Inhibitors identified through non-parametric cluster based permutation testing.

Connectivity analysis

Preliminary connectivity analyses between frontal and somatosensory brain regions did not reveal any significant correlation with MSNA. A deeper understanding and rationale behind the choice of connectivity measure used and investigating differences on a group level might be useful in a more detailed connectivity analysis in the future.

Whole brain analysis

In order to investigate whether other areas of the brain might be involved in the processing of the arousal response, we used non-parametric cluster-based permutation tests on the time-frequency responses over the whole brain. This analysis revealed only the Rolandic area as being significantly correlated with MSNA. However, this could be because cluster-based statistics are extremely sensitive to clusters that span large areas in time-frequency space; as such, true focal effects could go unnoticed in the presence of bigger clusters. A more refined approach to investigate focal effects in other brain regions is required for a thorough whole brain analysis.

3.3. RESULTS AND DISCUSSION

In this study, we presented a MEG experimental approach for investigating neural biomarkers for the MSNA response that can signify risk for later development of high blood pressure. We found a significant correlation between MSNA and spectral power changes in the ACC whereas no significant effect was found for the insular cortex. Both the ACC and insular cortex have been identified in the literature as brain centers for modulating sympathetic functions (Pool and Ransohoff, 1949, Oppenheimer et al., 1991, Oppenheimer et al., 1992, Craig, 2002, Critchley et al., 2003, Vogt and Derbyshire, 2009). In our study, the MSNA response profile reflects individuals' response strategies, and its correlation with ACC suggests that this brain region is involved in the evaluation and modulation of arousing stimuli, rather than just resting state sympathetic firing. These findings are in line with a previously reported role for the ACC that implicated its involvement in context-driven modulation of bodily arousal states (Critchley et al., 2003).

We also found a strong correlation between Rolandic beta rebound and MSNA that can serve as a biomarker for MSNA response profile. Beta rebound in response to somatosensory stimuli is a well-known phenomenon which is thought to represent 'idling' of cortical neurons (Pfurtscheller et al., 1996), an 'active inhibited state' (Cassim et al., 2001) or 'signaling status quo' (Engel and Fries, 2010). The correlation of beta rebound with the peripheral sympathetic arousal response may be a reflection of a response strategy wherein the brain prepares for defense by filtering out additional incoming information in the somatosensory cortex. Inhibitors with relatively higher beta rebound power for repetitive stimulation would therefore presumably have a stronger gating/filtering effect on new information in order to maintain the status quo of a fight-or-flight like response. In other words, it may be that Inhibitors block additional information by actively inhibiting or deactivating the cortex.

3.4. OUTLOOK

In the present study, one of the constraints in designing the protocol was to keep the MEG paradigm similar to the one used in previous microneurography studies, which is known to elicit a clear MSNA response. After identifying Rolandic beta as a biomarker, the paradigm could be redesigned in different ways to test how closely the beta rebound follows the MSNA response. For example, the 200 ms delay between the ECG R-wave and the stimulus is optimal for observing MSNA inhibition in microneurography. However, the timing of the stimulus might not affect the *cortical* response and/or the overall defense response strategy displayed in Inhibitors and non-Inhibitors. The current paradigm requires a long ISI (as much as 60 s) to maintain the arousing effect of the stimulation, which in turn leads to a rather long MEG scanning session, exhaustive to the volunteer subjects. Thus, it would be useful to study how closely the beta rebound in simple electrical stimulation responses with shorter ISI, without an arousal effect, is related to MSNA inhibition. This can further provoke questions such as do arousal induced MSNA transients reveal a much broader individual trait wherein some individuals have consistently high beta rebound filtering whereas others do not?

In this study we have collected rich dataset: in addition to MEG, we have EEG, MRI, Galvanic skin response, respiratory pattern, ECG, and pupil dilation data. For the scope of this study, we limited our analysis to the MEG data; however, analyzing, for example, the pupil response and heart rate variability in response to arousing stimuli would add to the understanding of the arousal response.

The analysis in this study was focused on oscillatory responses in selected ROIs. However, beyond that, one of the benefits of MEG is the ability to allow the study of the *interaction* between different brain regions. The ACC is known to modulate sympathetic control. Furthermore, based on the present study, we suggest that the Rolandic/somatosensory cortical brain response reflects the defense response strategy adopted by each individual. As such, the ACC might be modulating the somatosensory response. How this interaction is working can be investigated further via a more thorough connectivity analysis between these two regions than that which is presented herein and in Paper I. Moreover, investigating the mechanistic features of beta events, such as amplitude, number of events, etc., in single trial data might reveal additional information regarding the generators of the beta rhythm in both regions as suggested by a recent study (Sherman et al., 2016).

Partly due to the small number of subjects in this study, we limited our analysis to ROIs. An improved approach towards whole brain analysis, (remembering to exclude or otherwise mitigate the dominating effects of bigger clusters), could reveal more regions of interest that are involved in arousal processing. Understanding the arousal phenomenon, defense strategies, brain networks involved in the process, and their interaction remain important open research questions. Regardless, identifying a non-invasive biomarker for the MSNA response profile was a primary endpoint of this study that we successfully reached.

This study is a candidate clinical application involving both research and societal utilization of state-of-the-art MEG. MEG, in this study, has allowed us to expand our understanding of brain networks involved in sympathetic arousal and, more importantly, has identified a close relationship between an individual's sympathetic response and Rolandic beta rebound. However, utilizing these findings for assessing risk of hypertension in large populations or implementing them in a routine clinical screening is not feasible with state-of-art MEG systems. Fortunately, there are promising developments going on in the MEG world that could, in the future, lead to systems that are cheap and simple enough to be used clinically (i.e., like EEG systems are used today). Such hardware is best developed with clear applications in mind and validating their capabilities is critical to their clinical reach.

4 METHODS TO VALIDATE ON-SCALP MEG

New sensor technologies such as high-T_c SQUIDs and optically-pumped magnetometers (OPMs) present an opportunity for eliminating the need for liquid helium and reducing the standoff between the sensors and the head. Next generation MEG systems based on such sensor technologies could decrease maintenance costs and enable extraction of more information from the brain via what has now been termed “on-scalp MEG”. On-scalp MEG systems could then open new doors towards understanding of neural mechanism in the brain and provide a promising bridge between ECoG (invasive) and state-of-the-art (non-invasive) EEG and MEG. In this section, we present methods for validating the potential of single and multi-channel on-scalp MEG arrays.

4.1. INTRODUCTION

Researchers and clinicians started exploring clinical applications of MEG already in 1980s: even with a single channel MEG system, MEG provided valuable information regarding the location of epileptic activity long before full head systems were available on the market (Barth et al., 1982). However, routine clinical utilization of MEG for epilepsy investigations was slow to develop even though it showed remarkable improvement in presurgical epilepsy evaluations (Stefan et al., 2003, Knake et al., 2006, Knowlton et al., 2009, Fujiwara et al., 2012). MEG is today being used on clinical populations for understanding mechanisms and identifying biomarkers for neurodegenerative diseases like Parkinson's (Berendse and Stam, 2007, Stoffers et al., 2008) and Alzheimer's (Criado et al., 2007, Zamrini et al., 2011) as well as developmental disorders like Autism (Port et al., 2015), but primarily in the research setting. Clinical utilization of MEG has improved over time with the advancement in MEG hardware, software, and analysis tools; however the high installation and maintenance cost are still limiting factors for the MEG user-base growth (Van Veen et al., 1997, Taulu and Simola, 2006, Mantini et al., 2008, Oostenveld et al., 2011, Gramfort et al., 2014). Beyond cost, the software end of MEG has improved considerably in the last two decades, but analysis still requires investment and expertise. Improvement in the hardware has also been limited until recently when new sensor technologies began to show potential in MEG. On-scalp MEG systems, with such new sensor technologies, would not only be economical solutions, but the boost in the spatial resolution gained by coming closer to the head might, e.g., reduce the need for invasive ECoG-based investigations for epilepsy evaluation. In general, on-scalp MEG may bridge the gap between MEG being used for research on clinical populations to MEG being used routinely for clinical applications.

The path from proof-of-principle to clinical utilization is a long one. From the first MEG recording with a single SQUID in the 1970s, MEG hardware matured through 4-, 7-, 24-, 122-, and 300+-channel systems with full head coverage over the course of more than two decades (Romani et al., 1982, Lounasmaa et al., 1989, Ahonen et al., 1991, Foglietti et al., 1993, Knuutila et al., 1993, Pizzella et al., 2000, Okada et al., 2006). State-of-the-art MEG systems on the market today, based on low-T_c SQUID sensors, were, until recently, considered fully evolved and cutting edge in the field. Likewise, on-scalp MEG must embark on a similar, but entirely new journey of evolution from single-channel systems to a full-head system. However, this journey is

now guided by existing full-head MEG systems towards a better, perhaps simpler, and more economical solution.

One of the contending sensor technologies for next generation MEG systems are high-T_c SQUIDs. They operate at T=77 K and can therefore be cooled with liquid nitrogen, eliminating the use of liquid helium. This more moderate operating temperature means high-T_c sensor systems can suffice with a thermal insulation thickness of less than 1 mm between them and the room-temperature environment. High-T_c SQUID technology has always had potential for MEG; however, until recently, consistent sensor fabrication with sensitivity sufficient for MEG was a challenge. “High transition temperature SQUIDs for MEG” in (Körber et al., 2016) and a review by Faley et al. (Faley et al., 2017) discuss the current status of high-T_c SQUID technology and its potential for MEG systems.

The SQUID lab at Chalmers University is working towards the development of a high-T_c SQUID-based full-head MEG system. Starting in 2012 with a single channel system, they showed promising results by demonstrating sensitivity to well-known alpha and mu rhythms from the brain (Öisjöen et al., 2012). Six years later, a 7-channel system is now available (Pfeiffer et al., 2016). My contribution to this effort has been to develop protocols and benchmarking routines for validating and exploring the unique possibilities available to high-T_c sensor technology in on-scalp MEG recordings. As such, the long-term aim is to pave the way towards a high quality and economical neuroimaging system for clinical diagnostics.

4.1.1 On-scalp MEG recordings

The general on-scalp MEG experimental recording trend has followed that of the original MEG story: start with recording well-known neurophysiological signals (e.g., alpha rhythms), move towards those that could be of interest to researchers and clinicians (e.g., somatosensory evoked fields), and then explore areas where new information about the brain may be discovered. That trend also provides a natural learning curve for MEG recordings as one matures from quite simple experimental protocols to very complex ones that require months of planning together with neuroscientists and physiologists.

Several validation studies have already confirmed the ability of new sensor technologies, e.g., high-T_c SQUIDs and OPMs, to record brain activity (Öisjöen et al., 2012, Kim et al., 2014, Boto et al., 2017).

Benchmarking/validation recordings

With the sensitivity of the sensors with respect to brain activity established, more complex and quantitative recordings have been initiated. The aim of such benchmarking studies is to evaluate new sensor technology in comparison to existing systems (Paper II). An appropriate MEG protocol in this case would evoke a focal and robust response that does not habituate with repeated stimuli. The meaningful comparison between on-scalp and conventional MEG is related to source-to-sensor distance. The noise levels of new sensor technologies might not be as good as conventional low-T_c SQUIDs, however signal gain in on-scalp MEG is achieved by coming closer to the source. Focal responses are therefore preferred over diffuse sources/activations wherein the breadth of the activation can be larger than the relative change in source-to-sensor distance (and thus making the sensor comparison difficult to interpret). Moreover, a robust comparison experiment with a single channel system would require at least two runs of the stimulation/recording protocol in order to capture the negative and positive peak of the evoked response; the stability of the response with repeated stimulation is therefore critical. The N20 peak in the somatosensory area evoked by median nerve stimulation is a good example of such a response. It is a robust signal from a physiological prospective in the sense that it does not habituate (Desmedt and Tomberg, 1989, Tomberg et al., 1989). Many trails can therefore be averaged in order to boost the SNR. As it is an early response, the N20 can furthermore be detected with short inter-stimulus intervals. The overall duration of the protocol can therefore be short, even with many trials. The generator/source of the N20 is also quite focal which (in addition to allowing for a clear source-to-sensor estimation) simplifies modeling. The detailed experimental setup for benchmarking a single channel on-scalp high-T_c system is presented in Paper II.

Neuroimaging benefits of on-scalp MEG

Beyond benchmarking, an aim is to explore the potential neuroimaging benefit of on-scalp MEG. Recording the magnetic field from closer to the brain can potentially improve the spatial resolution of MEG. This might allow resolving and understanding micro-networks in the brain, e.g., gamma-band generators, or reveal new functional networks. For example, high amplitude theta band activity in the occipital region was discovered in one subject with single channel high-T_c MEG recordings (Öisjöen et al., 2012). Furthermore, we have observed unexpected features in MEG recordings of somatosensory evoked fields (Paper II).

4.2. EXPERIMENTAL SETUP

For single (or few) channel on-scalp MEG investigations, the existence of full-head MEG systems facilitates and guides the process. A full-head MEG system can be used to estimate the expected response at the cortical level and, as such, guide the search for optimal recoding locations for a single or few channel MEG system. The detailed protocol for benchmarking next generation on-scalp MEG systems to conventional systems is presented in Paper II. Here, the three general steps of the benchmarking recording process are summarized:

The first step is to run the whole stimulus paradigm with a full-head MEG system. This step not only validates the paradigm and confirms that the desired response is invoked, but also provides an estimated response profile for assisting single or multiple channel on-scalp recordings.

The second step is to estimate the expected neuromagnetic response on the scalp surface, for *a prior* selected time instant and brain region in order to guide the on-scalp recording locations. This step utilizes full head MEG data, as well as forward and inverse calculations that are discussed in more detail in the next section and chapter.

The third step is to identify/mark the scalp regions for optimally recoding the response and to adapt the paradigm according to the single (or multiple) channel recordings. This depends on the research question, the targeted response profile, and the available number of channels in the on-scalp MEG system. For example, for the N20 evoked field, if the aim is to compare only the gain in the amplitude from coming closer to the head with an on-scalp MEG system, then recording the maximum and minimum peak of the dipole response of the N20 peak (guided by the full head MEG measurements) might be sufficient. This would require running the MEG paradigm twice, as was done in Paper II. For the second benchmarking recording (discussed in the next section), the objective was to investigate the field pattern of the N20 response with a single channel on-scalp MEG system. In this case, recording from two positions was not enough. A grid of 20 to 25 locations covering the whole dipole field pattern of the N20 response would be an ideal recording protocol, but is not practical. Such a measurement would require 2 to 2.5 hours of measurement time only, excluding the time required for moving the single channel system from one measurement location to another. Moreover, habituation of the response over the course of such a long recording might become a concern. Therefore, recording from only a few locations on a line

connecting the positive peak, zero crossing, and negative peak of the N20 response was considered a suitable alternative.

4.3. ANALYSIS PIPELINE

To understand the steps involved in the analysis of benchmarking data, I present the analysis of the high-T_c recordings of the N20 peak of the somatosensory evoked magnetic field from our second benchmarking study (Andersen et al., 2017). The stimulus paradigm was electrical stimulation to the median nerve at the left wrist with a repetition rate of 2.8 Hz. The data was acquired through the NatMEG (dubbed the "low-T_c MEG") system and a single channel high-T_c SQUID based on-scalp MEG system. The stimulation protocol was repeated ten times to record the field at 10 different locations on the head (dictated by the full head low-T_c MEG recording) covering the line capturing the maximum, zero crossing, and the minimum of the N20-response for median nerve stimulation. Around 1000 stimuli (at least 5 minutes of recording) were delivered in each run. In the previous benchmarking experiments (reported in Paper II), we only recorded data from the maximum and minimum peaks. The results in Paper II indicated a more complex field pattern was detected by the high-T_c sensor recording as compared to that which was predicted from the conventional full-head MEG recordings. The aim of the second benchmarking recording, analyzed here, was to investigate those differences further. We have processed data from nine of ten recording locations here through the developed pipeline (one was rejected due to bad data quality).

The key steps in the data processing pipeline are:

1. Full head conventional MEG data is preprocessed following the regular MEG processing stream (as was explained in Chapter 2) and includes cleaning of the data, filtering, and estimating the sources of the recorded fields at time-points around the N20 peak.
2. The next step is to predict the magnetic field on the scalp surface for the time-points around the N20 peak. This could be done by forward projecting the source estimates from the low-T_c data to the head surface (Figure 8b), or extrapolating the field maps from the low-T_c helmet/sensors to the scalp surface (Figure 8c). The difference between these two approaches is that the fields predicted from estimated sources are regularized based on the assumptions made in the calculation of the inverse operator. Extrapolating the fields, on the other hand, is more sensitive to noise in the data as it consists only of translation of data from one sensor space to another. The low-T_c, and scalp-level magnetic activity estimates from each approach for the N20 peak are shown in Figure 8.

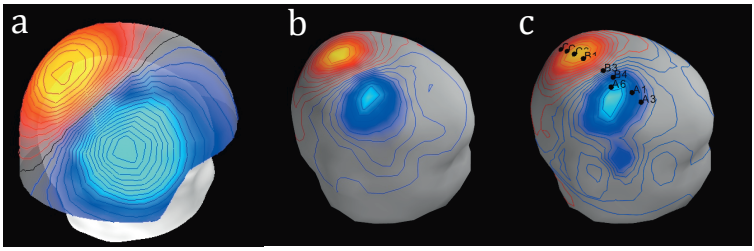

Figure 8. Different presentations of the MEG activity estimates for the N20 peak at time=21 ms. a) the neuromagnetic field at the low-T_c helmet surface. b) The field maps calculated by forward projecting the source estimates from the low-T_c data to the head surface. c) The field maps extrapolated from the low-T_c sensors to the scalp surface and marked with the points where high-T_c single channel data was recorded. The labels (left to right) C6, C1, C3 cover the positive peak, B1, B3, and B4 cover the zero crossing and A6, A1, and A3 cover the negative peak of the N20 response.

3. Identify the high-T_c on-scalp recording locations. The low-T_c sensors are fixed in a helmet shaped dewar. The position of the head with respect to this fixed sensor array is estimated based on the HPI coils attached to the head. As such, hundreds of fixed low-T_c sensors are used to localize the HPI coils and thus estimate the head position. For moveable single or multichannel systems the problem becomes more complicated. As shown by a recent simulation study, this can be solved for a small moveable multichannel system by estimating the sensor locations based on an array of HPI coils with known locations and orientations (Pfeiffer et al., 2018). For a single channel recording, the positions could roughly be estimated from digitizing the intended locations and aiming the sensors at those locations. In this case, a Polhemus FASTRAK (Polhemus, Colchester, Vermont) was used to digitize the aimed locations. However, human error and uncertainty in placement of the cryostat at the given location cannot be excluded. The magnetic field distribution of the N20 peak (projected from the low-T_c recordings), and markers of the high-T_c acquisition locations (C6, C1, C3, B1, B3, B4, A6, A1, A3) are shown in Figure 8c.

4. Extract the time courses for the predicted field at the scalp surface from the low-T_c data at the on-scalp recording locations (as shown in Figure 9).

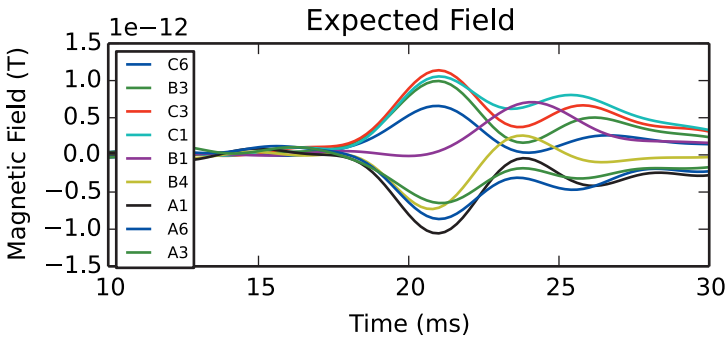

Figure 9. Expected/predicted on-scalp fields around the N20 activation, based on calculating the field maps on the scalp surfaces from the full-head low-T_c MEG recording. The predicted evoked response for each of the on-scalp MEG measurement positions (labels corresponding to those in Figure 8), based on the field extrapolation approach, are presented.

5. The high-T_c data is preprocessed with the same parameters (filters, etc.) as the low-T_c data was. The high-T_c recorded fields are shown in Figure 10.

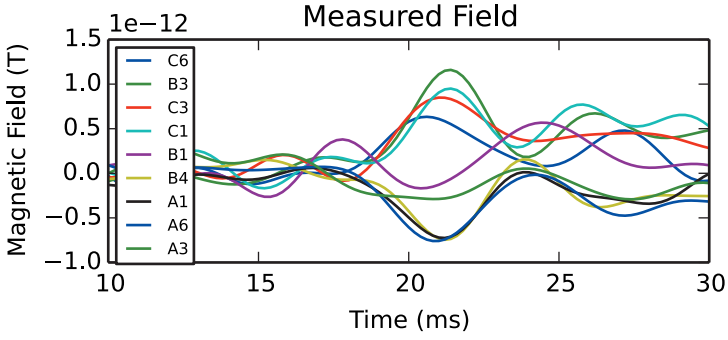

Figure 10. Measured fields from the single channel high-T_c on-scalp recording of the somatosensory evoked fields around the N20 activation. Labels A1-C6 correspond to those in Figures 8 and 9.

6. The last step in this pipeline is to investigate the differences in the measured high-T_c and low-T_c data. The recorded fields can be visualized in different formats/maps for better understanding. For example, contour maps for the predicted and measured on-scalp fields are shown in Figure 11.

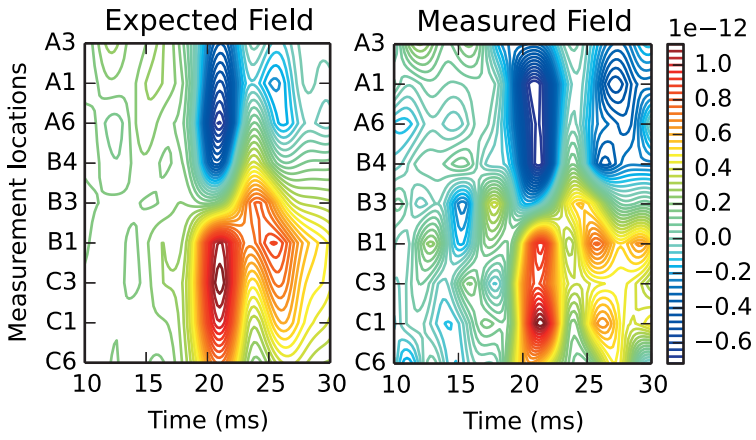

Figure 11. The contours maps of the expected (conventional, low-T_c MEG) and measured (single channel high-T_c on-scalp) fields.

The contours in the expected field in Figure 11 indicate a single dipole pattern at t=21 ms. At t=26 ms the pattern is more spatially diffuse indicating a larger cortical area of activation, but still a roughly dipolar pattern. The measured field is more complex. At t=21 ms, the positive and negative peaks in the field pattern, each contain two peaks that add up. At t=26 ms, those double-peaks patterns are more distinct.

The simple difference between measured and predicted data sets is presented in Figure 12. Such a presentation can provide insights into the types of sources to which on-scalp MEG is more—or even uniquely—sensitive, as compared to conventional MEG. The field pattern in the contour map of the difference suggests a more complicated source generated signals at the scalp surface than that which would be generated by a simple dipole; the source is, however, of very low amplitude, especially compared to the predicted N20 component. The next step would be to localize these differential field patterns in order to investigate if on-scalp measurements are able to reveal additional sources as compared to conventional MEG. This might indicate improved spatial resolution is possible with a high-T_c on-scalp system as compared to the state-of-the-art.

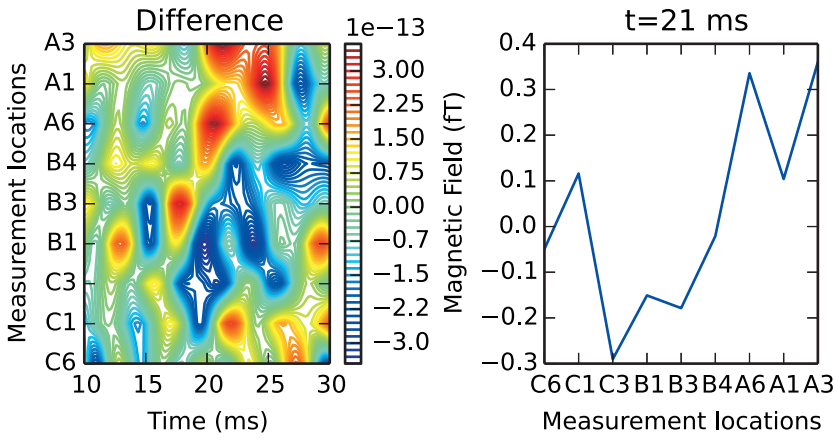

Figure 12. The difference between measured and expected fields. Left: the full time-course of the measured field that is in excess of the predicted one. Right: the difference between measured and expected field for one time instant (t=21ms). These visualizations of the differential activity indicate more complicated field patterns were detected at the scalp surface than that which is expected from a single dipole for the N20 response.

4.4. OUTLOOK

The long-term goal is to develop a full head on-scalp MEG system. However, the multi-channel systems developed with new sensor technologies could already be used in preclinical and clinical applications. The pipeline and set-up presented in this chapter would facilitate such recordings. Single or multi-channel systems could be used in an application where investigating a region of interest is of more relevance than the localization of all activity. For example, few-channel on-scalp MEG investigations of an epileptogenic zone intended to provide additional information about its location and extent could be guided by, for example, EEG localization. A preclinical investigation of mechanisms promoting hypertension based on individuals' arousal responses (e.g. with a biomarker already identified to be generated in the Rolandic area) could be another application area. On-scalp MEG systems with limited channel count could also contribute towards the understanding of more complicated neural mechanism in the brain. Some examples of this include investigating local communication within cortical layers in the primary visual and/or auditory cortices or attempting to identify feedforward and feedback networks between cortical layers (Troebinger et al., 2014, Michalareas et al., 2016).

5 FRAMEWORK FOR DESIGNING ON-SCALP MEG ARRAYS

Single and multichannel recordings provide a proof of concept that new sensor technologies can be used for MEG. However, such recordings fail to demonstrate the neuroimaging advantage of new sensor technologies in full-head systems as compared to the state-of-the-art. An evaluation of the performance of new sensors in realistic full-head arrays is important both for demonstrating their advantages over today's MEG systems theoretically, but also in the practical design of next generation neuroimaging systems. In this work, I have developed a framework for evaluating the performance of new sensor technologies in a full head system, with varying layouts and design parameters such as sensor dimensions, standoff from the head, center-to-center distance, etc.

5.1. INTRODUCTION

In conventional MEG, the heavy cryogenic requirements of low-T_c SQUIDs did not allow for much flexibility in designing full head systems. The only practical choice was to densely pack low-T_c sensors in a single dewar that provides the vacuum insulation for the sensors. The low operating temperature of low-T_c SQUIDs (less than 10K) requires thermal insulation of around 2 cm from the sensors to room temperature. New sensor technologies eliminate the use of liquid helium and hence the bulky cooling system. The two most promising sensor technologies contending for next generation MEG systems are OPMs and high-T_c SQUIDs. OPMs do not require cryogenics at all: the sensors instead operate above room temperature and require insulation to prevent heat conduction to the head surface. For high-T_c based systems, the use of liquid nitrogen or even cryogen-free micro-cooling technologies instead of helium has allowed a lot more flexibility and options in designing sensor layouts for next generation systems.

Theoretical studies evaluating the performance of new sensor technologies are already present in the literature (Nenonen et al., 2004, Schneiderman, 2014, Boto et al., 2016, Iivanainen et al., 2016). These simulation studies have used hypothetical sensor layouts to compare the potential performance of new technologies with the state-of-the-art. The layouts are often created by snapping the sensor locations of current MEG systems to the head surface; as such the array layouts are arbitrary and restricted to the number of sensors in the current MEG system. Realistic array designs for full head systems that exploit the full potential of on-scalp technology are still lacking. Moreover, the layouts that have heretofore been explored are focused on a customized array that is adaptable to each individual's head. The idea is very appealing in theory; however, practical constraints (such as the size of individual sensor module) will directly affect how well the sensors cover the head. Evaluating the tradeoff between flexibility and coverage is therefore needed: there could be other design approaches that can provide better average coverage even if they are not fully customizable to an individual's head shape.

In our study, we have assessed three design approaches for full-head systems:

1. Adaptable system consisting of single sensor units, which adapt to individual's head shape (similar to EEG caps).

2. Conventional layout in which sensors are tightly and inflexibly packed in a helmet-shaped dewar (similar to state-of-the-art MEG systems).

3. A modular design, in which multiple sensors are tightly and inflexibly packed in one unit (e.g., a cryostat), and several such units are arranged around the head to provide full head coverage. This approach is, in principle, somewhere between fully adaptable customized systems and a fixed rigid dewar.

For assessing the performance of different MEG sensor array layouts, information capacity is a useful comparison metric (Nenonen et al., 2004, Schneiderman, 2014, Boto et al., 2016, Iivanainen et al., 2016). Information capacity is simple to calculate and quantifies the sensor distances from the sources, sensitivity, and configuration into a single number. However, different layout configurations of sensors can give different coverage of the head. Quantifying these differences in coverage is not possible with information capacity alone as its gives the total information extracted from the entire brain (assuming all sources in the brain are active at the same time); as such, the spatial dimension is lost. Other metrics allow comparisons of spatial coverage, for example, via the point spread function (PSF) and its derivatives peak position error (which estimates the localization accuracy based on the correlation scores of neighboring sources), and cortical area (number of sources exceeding a certain correlation score). However, these all require calculation of an inverse operator and are hence strongly affected by the various choices/assumptions made to calculate it. Relative sensitivity cortical maps are based only on the lead field (no inverse operator is required); however, they do not account for differences in the noise levels of different kind of sensors being compared. This is an important limitation, as on-scalp MEG sensors generally have higher noise levels than their low-T_c counterparts. To this end, we have introduced a new method that combines information capacity with spatial information, namely Spatial Information Density (SID), as presented in Paper III. SID evaluates the information content by treating each cortical source independently; as such, it quantifies the total information extracted by a given sensor array from each patch of the cortex. By displaying SID on the cortical level, one can therefore understand which brain regions are well-sampled by a given sensor array, and which are not.

The performance of a given MEG system is affected by many parameters such as the sensitivity of the sensors (noise levels), packing density of the sensors (center-to-center distance), number of sensors, and how far the sensors are from the scalp surface (standoff). These parameters are also partially

dependent on one another (e.g., the center-to-center distance and standoff roughly dictate the number of sensors) and on the sensor technology under study. To have a better idea of how these parameters interact and for designing an optimal layout for next generation MEG system, we have developed a framework that allows designing different arrays with variable sensor configurations and estimating their performance in terms of known evaluation metrics.

5.2. FRAMEWORK

The framework is developed in MATLAB and python, following the standard formats and coordinate systems used in the MNE toolbox for MEG data processing. Defining the sensor arrays in a standard MEG format allows users to benefit from the functionality of the toolboxes (such as calculation of PSFs, sensitivity maps, simulating MEG data for different array designs, etc.)

The main modules in the framework are as follows:

Designing the array

The first module distributes the sensors on the head (or helmet) surface according to the chosen design parameters. The output of this module is the locations and orientations of the sensors in an array, maintaining specific center-to-center distance and standoff from the given head or helmet surface.

For uniformly distributing the sensors on a head or helmet surface, we implemented a Chebyshev net algorithm in MATLAB that generates a roughly square grid on a curved surface as shown in Figure 13. The Chebyshev net is based on finding the points of intersection of circles with fixed radii (the radius is equal to the required grid length) along two perpendicular primary axes that are chosen semi-arbitrarily (typically front-to-back and left-to-right in the head coordinate system). More detail about this meshing method is explained in (Popov, 2002). An example of a Chebyshev net on a helmet surface is shown in Figure 13.

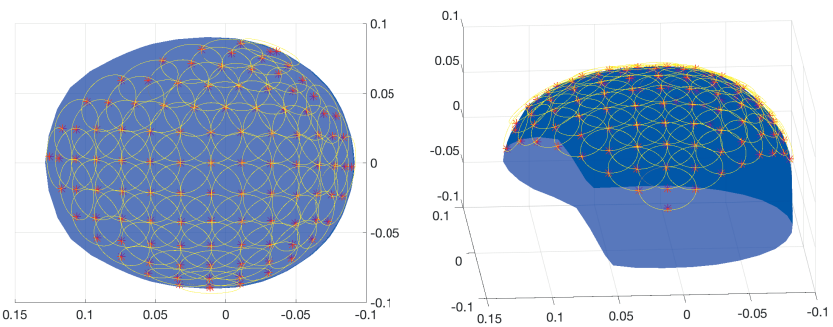

Figure 13. A Chebyshev grid on a helmet surface. The red asterisk shows the identified grid locations through the Chebyshev algorithm based on the intersection of fixed-radius (yellow-colored) circles projected onto the curved surface of the helmet (blue).

The program allows the user to specify the surface (head or helmet), standoff from the surface for placing sensors, and center-to-center spacing of the grid points (i.e. the sensor locations). The sensors are then uniformly distributed according to those parameters.

For designing the layout for the modular system approach, a GUI-based program has been developed. The user is prompted to manually select the locations of the unit (e.g. cryostat) around the head surface. The program calculates the locations and orientations of the sensors within the unit and with respect to the head while ensuring the all sensors are no closer to the head than the minimum standoff specified.

Aligning the sensor array with the head model

To make the sensor arrays compatible with the MNE toolbox, this module aligns and transforms the coordinate system according to the MNE format. The sensor arrays are defined in device coordinates, and head models are defined in MRI coordinates. All transformations between these coordinate frames are calculated at this step. The coordinate systems used in the MNE toolbox for defining the MEG sensor array and MRI data for the head model are explained in detail in the MNE user manual (Hämäläinen, 2005).

Forward/gain matrix calculation

In this module, all transformations and sensor specifications are written in a fif-file format (a standard MEG data format) using standard MNE toolbox functions. Once the fif-files are created the arrays can be used with any MEG analysis toolbox. The forward/gain matrix is calculated following the standard MEG data processing pipeline.

Evaluating performance based on different metrics

The sensor arrays generated can be evaluated and compared with different evaluation metrics. MATLAB code is developed to calculate the total information content and SID maps based on the calculation presented in Paper III. Other metrics, e.g., sensitivity maps and PSFs, are already implemented in available open source MEG toolboxes. This framework is generalized and can be used to approximate design parameters for different sensor technologies.

An example of semi-idealized MEG sensor arrays

In order to investigate the effects of some of the most important aspects of MEG performance, we simulated a range of design variables and compared

them with this framework. Sensor standoff, packing density, and noise were varied through what is reasonably achievable with todays sensor technology. This approach is particularly powerful as semi-idealized systems can be compared irrespective of the constraints associated with sensor technology used: we simulated arrays of point magnetometers that can thus be distributed with arbitrary density. The point magnetometers are distributed on the scalp surface of an average head model provided by the FreeSurfer toolbox, with three different standoffs, three different noise levels and varying center-to-center distance. The three standoffs are chosen to represent the three competing sensor technologies available in the market: 1 mm for high-T_c SQUID sensors (Öisjöen et al., 2012), 6 mm for OPM sensors (QuSpin QZFM), and 20 mm for low-T_c SQUID sensors (Elekta Neuromag® TRIUX). The noise levels used in the simulations are 50 fT/√Hz (a pessimistic noise estimate for mass-produced high-T_c SQUID technology), 11 fT/√Hz (demonstrated by both OPMs and high-T_c SQUID technologies), and 3 fT/√Hz (typical for low-T_c technology). The results (presented in Figure 14) show that even sensors with relatively high noise levels could still perform better in full-head MEG because of the reduced standoff and denser packing, indicating the benefit of the smaller standoff in on-scalp MEG.

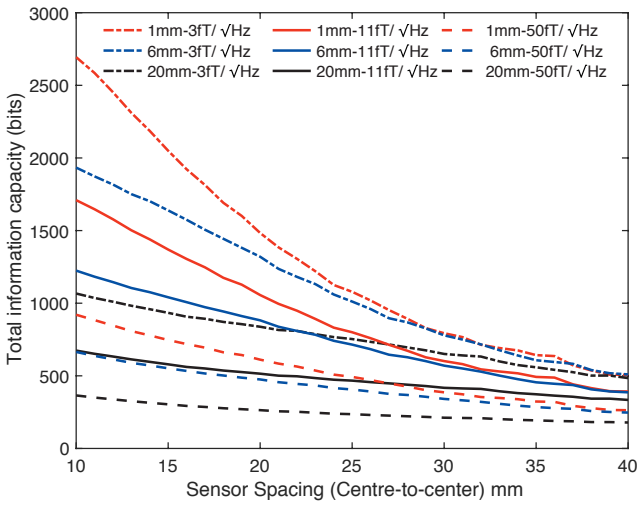

Figure 14. Total information capacity for point magnetometers distributed around the scalp surface of the average FreeSurfer head with variable center-to-center spacing. The legend indicates the sensor-to-head distance and sensor white noise level for each curve.

5.2.1 Evaluation of practical high-T_c SQUID based MEG arrays

To evaluate the potential of high-T_c SQUID sensors for next generation MEG systems, we designed three practical layouts based on realistic design parameters for high-T_c SQUIDs in Paper III. The layouts were compared to the low-T_c SQUID-based Elekta Neuromag system. The comparisons were based on the traditional Information content metric and the coverage of the arrays was evaluated with the new method developed, i.e., SID. Moreover, additional benefits of on-scalp MEG for children was also explored in Paper III.

5.3. OUTLOOK

The developed framework can be used to design and explore a wide variety of high-T_c SQUID-based layouts. For example, we evaluated the optimum number of channels per cryostat in a modular cryostat approach, i.e., with more than 7 sensors in each module (Boldizar and Slipac, 2017). The framework could further be used for optimizing sensor size. In the future, it could be integrated into open source MEG toolboxes, allowing other sensor technologies, like OPMs, to benefit from the developed pipelines.

The SID method presented in Paper III is a practical approach to assess the coverage of different sensor arrays in terms of neuroimaging on the cortical surface. However SID treats the sources independently by estimating how much information an array extracts from a single source when only that source is active. Total information capacity, on the other hand, estimates the amount of information an array can extract when all sources in the brain are activated. These approaches thus cover the extreme ends of information flow from sources to sensors; both of them are likely to be too simplistic. A more realistic approach could be to cater for the brain noise, that is, to estimate how the detection of a source would be affected if the neighboring sources are active but not contributing to the signal of interest. Other methods, such as peak position error, give some estimate of the interaction of neighboring sources by measuring the correlation scores of the lead field of the active source with the rest of the brain. As with many metrics, however, it does not account for sensor noise, which as we have seen, is a critical parameter for MEG systems. A new method that models both the information from each source and brain noise might lead to a better estimator of the true neuroimaging sensitivity of MEG systems.

6 SUMMARY

This thesis adds a few steps on the path towards making a non-invasive functional neuroimaging system with high spatiotemporal resolution clinically available to large populations. Currently, MEG appears to be the most promising modality, given its high spatiotemporal resolution. In this work, we presented methods that bridge the gap between conventional low-T_c MEG today and next generation on-scalp MEG that has the potential to become a clinically used diagnostic method in the future.

In the arousal study, we developed an experimental approach for a new conventional MEG-based clinical application and identified cortical biomarkers for predicting risk for cardiovascular disease, a major clinical focus worldwide. A 20-subject study and analysis pipelines were implemented. The most prominent neural correlates of MSNA responses to arousal were investigated, yielding insight into how incoming arousing sensory information in the brain is differentially processed in healthy individuals, which may reflect a spectrum of defense strategies.

We also present methods for guiding the development of next generation helium-free MEG systems with improved spatial resolution. For the validation studies, a pipeline to analyze single channel data (or a few multichannel sensor arrays) was developed. The data recorded with high-T_c sensor technology was compared to conventional MEG recordings. Systematic benchmarking routines were developed for exploring the neuroimaging benefit of on-scalp MEG. To assess the potential of a full-head on-scalp MEG system, a theoretical framework for guiding design parameters (like packing density, pickup loop size, etc.) of sensor arrays was presented with information capacity as a standard evaluation metric. To assess the coverage and spatial dimension of information content, a new metric, SID, was introduced. Realistic high-T_c SQUID-based sensor layouts were evaluated and compared to a conventional MEG system using adult and child head models.

In the future, the 7-channel on-scalp MEG system developed at Chalmers University should be used for research and clinical assessment of cardiovascular risk. The brain region and biomarker we established with conventional MEG recordings i.e., the Rolandic beta rebound, can furthermore be targeted with the 7-channel system for developing potential therapeutic interventions. The benchmarking pipeline and framework presented in this thesis can guide such on-scalp MEG recordings while the theoretical framework, particularly

SID, can guide optimal cryostat placement (see Cover Illustration for an example).

ACKNOWLEDGEMENTS

Four years ago, I started my PhD studies aiming for a doctorate degree, but my arduous uphill journey gave me much more at the end. I made remarkable friends, found exceptional mentors, and gathered priceless memories. I was fortunate during my tenure to have met people who motivated me to excel and stood by my side at every turn. Sumptuous monthly MEG dinners, exhilarating board game nights, earnest chats and discussions in offices and corridors, lunch break gossips at MTW, fierce discussion over fika, sharing experiences, and having so many people around that really cared made these four years a journey worth remembering.

I am very grateful to my supervisor and extraordinary teacher Justin Schneiderman. Your unflinching commitment to the MEG group and hard work has been an inspiration and source of motivation for me to bring out my best. Your support, guidance, and patience made my PhD possible.

I am indebted to my co-supervisor and mentor, Mikael Elam. Your motivation and encouragement have been invaluable throughout. Thank you for making complicated tasks accessible and challenges effortless and manageable for me.

I would also like to take this opportunity to thank Elena for her tremendous support throughout my tenure. I have learnt so much from you. My untimely intrusions to your office with new results and your remarkable instant insights have gone a long way to help me.

My special thanks go to the SQUID SQUAD: Christoph, Elin, Silvia, Minshu, Sobhan, John, and Darko. I consider myself fortunate to have worked with such a friendly, lively, and zealous group. You guys are simply the best.

I would like to express my gratitude to Moa. Even though we have only worked together for a year, your support has been invaluable.

Thank you Johan for your profound discussions and coding insights.

I am grateful to all my friends and esteemed colleagues at MedTech West especially Helene, Simon, Muhammad, Markus, Emily, Niklas, Alvin, Jennifer, Agnes, Kerstin, Emilia, Leif, Rolf, and Henrik.

Special thanks to Amandine for your love and support and making my stay in Boston memorable. Thank you Kestas and Nouchine for giving me an opportunity to visit your lab and thank you Cody for your valuable time.

I am indebted to my two special friends: Mitra and Sabiha. You provided me with a home away from home. Your kindness, generosity, and warmth are ineffable. Thank you for being my family in Gothenburg.

I would also like to thank Eileen and Emil and all my friends in Sweden.

I would like to dedicate this thesis to my parents. I am humbled by their love, unconditional support, and unstaggering faith in me. Lastly, I would like to thank my brother and sisters for always challenging me to seek out my limits and potential.

I would finally like to thank the Boehringer Ingelheim Fund for the visiting grant to the Martinos Center for Biomedical Imaging, Boston, which gave me the opportunity to learn from the experts and make new friends.

REFERENCES

Ahonen A, Hamalainen M, Kajola M, Knuutila J, Lounasmaa O, Simola J, Tesche C, Vilkman V (1991) Multichannel SQUID systems for brain research. *IEEE Transactions on Magnetics* 27:2786-2792.

Andersen LM, Oostenveld R, Pfeiffer C, Ruffieux S, Jousmäki V, Hämäläinen M, Schneiderman JF, Lundqvist D (2017) Similarities and differences between on-scalp and conventional in-helmet magnetoencephalography recordings. *PLoS One* 12:e0178602.

Asahina M, Suzuki A, Mori M, Kanesaka T, Hattori T (2003) Emotional sweating response in a patient with bilateral amygdala damage. *International Journal of Psychophysiology* 47:87-93.

Baillet S (2017) Magnetoencephalography for brain electrophysiology and imaging. *Nature Neuroscience* 20:327.

Barth DS, Sutherling W, Engel J, Beatty J (1982) Neuromagnetic localization of epileptiform spike activity in the human brain. *Science* 218:891-894.

Bechara A, Tranel D, Damasio H, Adolphs R, Rockland C, Damasio AR (1995) Double dissociation of conditioning and declarative knowledge relative to the amygdala and hippocampus in humans. *Science* 269:1115-1118.

Benarroch EE (1993) The central autonomic network: functional organization, dysfunction, and perspective. In: Mayo Clinic Proceedings, vol. 68, pp 988-1001: Elsevier.

Berendse HW, Stam CJ (2007) Stage-dependent patterns of disturbed neural synchrony in Parkinson's disease. *Parkinsonism & Related Disorders* 13:S440-S445.

Boldizar F, Slipac U (2017) Optimizing design of on-scalp MEG systems. *Master Thesis at Chalmers University of Technology*.

Boto E, Bowtell R, Krüger P, Fromhold TM, Morris PG, Meyer SS, Barnes GR, Brookes MJ (2016) On the potential of a new generation of magnetometers for MEG: a beamformer simulation study. *PLoS One* 11:e0157655.

Boto E, Meyer SS, Shah V, Alem O, Knappe S, Kruger P, Fromhold TM, Lim M, Glover PM, Morris PG (2017) A new generation of magnetoencephalography: room temperature measurements using optically-pumped magnetometers. *Neuroimage* 149:404-414.

Cassim F, Monaca C, Szurhaj W, Bourriez J-L, Defebvre L, Derambure P, Guieu J-D (2001) Does post-movement beta synchronization reflect an idling motor cortex? *Neuroreport* 12:3859-3863.

Cohen D, Cuffin BN, Yunokuchi K, Maniewski R, Purcell C, Cosgrove GR, Ives J, Kennedy JG, Schomer DL (1990) MEG versus EEG localization test using implanted sources in the human brain. *Annals*

of Neurology: Official Journal of the American Neurological Association and the Child Neurology Society 28:811-817.

Craig AD (2002) How do you feel? Interoception: the sense of the physiological condition of the body. *Nature Reviews Neuroscience* 3:655-666.

Criado JR, Amo C, Quint P, Kurelowech L, Otis SM (2007) Using magnetoencephalography to study patterns of brain magnetic activity in Alzheimer's disease. *American Journal of Alzheimer's Disease & Other Dementias®* 21:416-423.

Critchley HD, Corfield D, Chandler M, Mathias C, Dolan RJ (2000) Cerebral correlates of autonomic cardiovascular arousal: a functional neuroimaging investigation in humans. *The Journal of Physiology* 523:259-270.

Critchley HD, Mathias CJ, Josephs O, O'doherty J, Zanini S, Dewar BK, Cipolotti L, Shallice T, Dolan RJ (2003) Human cingulate cortex and autonomic control: converging neuroimaging and clinical evidence. *Brain* 126:2139-2152.

Dale AM, Fischl B, Sereno MI (1999) Cortical surface-based analysis: I. Segmentation and surface reconstruction. *Neuroimage* 9:179-194.

Dale AM, Liu AK, Fischl BR, Buckner RL, Belliveau JW, Lewine JD, Halgren E (2000) Dynamic statistical parametric mapping: combining fMRI and MEG for high-resolution imaging of cortical activity. *Neuron* 26:55-67.

Damasio A, Tranel D, Damasio H Somatic Markers and the Guidance of Behavior: Theory and Preliminary Testing. Frontal Lobe Function and Dysfunction. Edited by: S. Levin H, Eisenberg HM, Benton AL. 1991. New York, Oxford University Press.

Delius W, Hagbarth KE, Hongell A, Wallin B (1972) General characteristics of sympathetic activity in human muscle nerves. *Acta Physiologica* 84:65-81.

Della Penna S, Pizzella V, Cianflone F, Del Gratta C, Erné S, Granata C, Naddeo A, Russo M, Romani G (2003) A 500 Channel Neuromagnetometer. *Applied Superconductivity* 3311-3316.

Desmedt JE, Tomberg C (1989) Mapping early somatosensory evoked potentials in selective attention: critical evaluation of control conditions used for titrating by difference the cognitive P30, P40, P100 and N140. *Electroencephalography and Clinical Neurophysiology/Evoked Potentials Section* 74:321-346.

Donadio V, Kallio M, Karlsson T, Nordin M, Wallin BG (2002a) Inhibition of human muscle sympathetic activity by sensory stimulation. *The Journal of Physiology* 544:285-292.

Donadio V, Karlsson T, Elam M, Wallin BG (2002b) Interindividual differences in sympathetic and effector responses to arousal in humans. *The Journal of Physiology* 544:293-302.

Donadio V, Liguori R, Elam M, Karlsson T, Giannoccaro M, Pegenius G, Giambattistelli F, Wallin B (2012) Muscle sympathetic response to arousal predicts neurovascular reactivity during mental stress. *The Journal of Physiology* 590:2885-2896.

Eder DN, Elam M, Wallin BG (2009) Sympathetic nerve and cardiovascular responses to auditory startle and prepulse inhibition. *International Journal of Psychophysiology* 71:149-155.

Edwards L, Inui K, Ring C, Wang X, Kakigi R (2008) Pain-related evoked potentials are modulated across the cardiac cycle. *PAIN*® 137:488-494.

Edwards L, McINTYRE D, Carroll D, Ring C, Martin U (2002) The human nociceptive flexion reflex threshold is higher during systole than diastole. *Psychophysiology* 39:678-681.

Engel AK, Fries P (2010) Beta-band oscillations—signalling the status quo? *Current Opinion in Neurobiology* 20:156-165.

Faley M, Dammers J, Maslennikov Y, Schneiderman J, Winkler D, Koshelets V, Shah N, Dunin-Borkowski R (2017) High-Tc SQUID biomagnetometers. *Superconductor Science and Technology* 30:083001.

Fischl B, Sereno MI, Dale AM (1999) Cortical surface-based analysis: II: inflation, flattening, and a surface-based coordinate system. *Neuroimage* 9:195-207.

Foglietti V, Pasquarelli A, Pizzella V, Torrioli G, Romani G, Casciardi S, Gallagher W, Ketchen M, Kleinsasser A, Sandstrom R (1993) Operation of a hybrid 28-channel neuromagnetometer. *IEEE Transactions on Applied Superconductivity* 3:1890-1893.

Forouzanfar MH, Alexander L, Anderson HR, Bachman VF, Biryukov S, Brauer M, Burnett R, Casey D, Coates MM, Cohen A (2015) Global, regional, and national comparative risk assessment of 79 behavioural, environmental and occupational, and metabolic risks or clusters of risks in 188 countries, 1990–2013: a systematic analysis for the Global Burden of Disease Study 2013. *The Lancet* 386:2287-2323.

Fujiwara H, Greiner HM, Hemasilpin N, Lee KH, Holland-Bouley K, Arthur T, Morita D, Jain SV, Mangano FT, Rose DF (2012) Ictal MEG onset source localization compared to intracranial EEG and outcome: improved epilepsy presurgical evaluation in pediatrics. *Epilepsy Research* 99:214-224.

Gianaros PJ, Van der Veen FM, Jennings JR (2004) Regional cerebral blood flow correlates with heart period and high‐frequency heart period variability during working‐memory tasks: Implications for the cortical and subcortical regulation of cardiac autonomic activity. *Psychophysiology* 41:521-530.

Gramfort A, Luessi M, Larson E, Engemann DA, Strohmeier D, Brodbeck C, Goj R, Jas M, Brooks T, Parkkonen L (2013) MEG and EEG data analysis with MNE-Python. *Frontiers in Neuroscience* 7:267.

Gramfort A, Luessi M, Larson E, Engemann DA, Strohmeier D, Brodbeck C, Parkkonen L, Hämäläinen MS (2014) MNE software for processing MEG and EEG data. *Neuroimage* 86:446-460.

Gray MA, Rylander K, Harrison NA, Wallin BG, Critchley HD (2009) Following one's heart: cardiac rhythms gate central initiation of sympathetic reflexes. *Journal of Neuroscience* 29:1817-1825.

Hämäläinen M (2005) MNE software user's guide. *NMR Center, Mass General Hospital, Harvard University* 58:59-75.

Hämäläinen MS, Ilmoniemi RJ (1994) Interpreting magnetic fields of the brain: minimum norm estimates. *Medical and Biological Engineering and Computing* 32:35-42.

Hansen P, Kringelbach M, Salmelin R (2010) MEG: an introduction to methods: Oxford university press.

Hari R, Salmelin R (2012) Magnetoencephalography: from SQUIDs to neuroscience: Neuroimage 20th anniversary special edition. *Neuroimage* 61:386-396.

Hyvärinen A, Oja E (2000) Independent component analysis: algorithms and applications. *Neural Networks* 13:411-430.

Iivanainen J, Stenroos M, Parkkonen L (2016) Measuring MEG closer to the brain: Performance of on-scalp sensor arrays. *Neuroimage*.

Kim K, Begus S, Xia H, Lee S-K, Jazbinsek V, Trontelj Z, Romalis MV (2014) Multi-channel atomic magnetometer for magnetoencephalography: A configuration study. *Neuroimage* 89:143-151.

Knake S, Halgren E, Shiraishi H, Hara K, Hamer H, Grant P, Carr V, Foxe D, Camposano S, Busa E (2006) The value of multichannel MEG and EEG in the presurgical evaluation of 70 epilepsy patients. *Epilepsy Research* 69:80-86.

Knowlton RC, Razdan SN, Limdi N, Elgavish RA, Killen J, Blount J, Burneo JG, Ver Hoef L, Paige L, Faught E (2009) Effect of epilepsy magnetic source imaging on intracranial electrode placement. *Annals of Neurology: Official Journal of the American Neurological Association and the Child Neurology Society* 65:716-723.

Knuutila JE, Ahonen AI, Hamalainen M, Kajola MJ, Laine PP, Lounasmaa O, Parkkonen L, Simola J, Tesche C (1993) A 122-channel whole-cortex SQUID system for measuring the brain's magnetic fields. *IEEE Transactions on Magnetics* 29:3315-3320.

Körber R, Storm J-H, Seton H, Mäkelä JP, Paetau R, Parkkonen L, Pfeiffer C, Riaz B, Schneiderman JF, Dong H et al., (2016) SQUIDs in biomagnetism: a roadmap towards improved healthcare. *Superconductor Science and Technology* 29:113001.

Lounasmaa O, Hari R, Joutsiniemi S-L, Hämäläinen M (1989) Multi-SQUID recordings of human cerebral magnetic fields may give information about memory processes. *EPL (Europhysics Letters)* 9:603.

Macefield VG, Taylor JL, Wallin BG (1998) Inhibition of muscle sympathetic outflow following transcranial cortical stimulation. *Journal of the Autonomic Nervous System* 68:49-57.

Mantini D, Franciotti R, Romani GL, Pizzella V (2008) Improving MEG source localizations: an automated method for complete artifact removal based on independent component analysis. *Neuroimage* 40:160-173.

Maris E, Oostenveld R (2007) Nonparametric statistical testing of EEG-and MEG-data. *Journal of Neuroscience Methods* 164:177-190.

Michalareas G, Vezoli J, Van Pelt S, Schoffelen J-M, Kennedy H, Fries P (2016) Alpha-beta and gamma rhythms subserve feedback and feedforward influences among human visual cortical areas. *Neuron* 89:384-397.

Nenonen J, Kajola M, Simola J, Ahonen A (2004) Total information of multichannel MEG sensor arrays. In: Proceedings of the 14th international conference on biomagnetism (Biomag2004), pp 630-631.

Öisjöen F, Schneiderman JF, Figueras G, Chukharkin M, Kalabukhov A, Hedström A, Elam M, Winkler D (2012) High-T c superconducting quantum interference device recordings of spontaneous brain activity: Towards high-T c magnetoencephalography. *Applied Physics Letters* 100:132601.

Okada Y, Pratt K, Atwood C, Mascarenas A, Reineman R, Nurminen J, Paulson D (2006) BabySQUID: a mobile, high-resolution multichannel magnetoencephalography system for neonatal brain assessment. *Review of Scientific Instruments* 77:024301.

Olesen J, Gustavsson A, Svensson M, Wittchen HU, Jönsson B, Group CS, Council EB (2012) The economic cost of brain disorders in Europe. *European Journal of Neurology* 19:155-162.

Oostenveld R, Fries P, Maris E, Schoffelen J-M (2011) FieldTrip: open source software for advanced analysis of MEG, EEG, and invasive electrophysiological data. *Computational Intelligence and Neuroscience* 2011:1.

Oppenheimer SM, Gelb A, Girvin JP, Hachinski VC (1992) Cardiovascular effects of human insular cortex stimulation. *Neurology* 42:1727-1727.

Oppenheimer SM, Wilson JX, Guiraudon C, Cechetto DF (1991) Insular cortex stimulation produces lethal cardiac arrhythmias: a mechanism of sudden death? *Brain Research* 550:115-121.

Park H-D, Correia S, Ducorps A, Tallon-Baudry C (2014) Spontaneous fluctuations in neural responses to heartbeats predict visual detection. *Nature Neuroscience* 17:612-618.

Pfeiffer C, Andersen LM, Lundqvist D, Hämäläinen M, Schneiderman JF, Oostenveld R (2018) Localizing on-scalp MEG sensors using an array of magnetic dipole coils. *PLoS One* 13:e0191111.

Pfeiffer C, Ruffieux S, Schneiderman J, Chukharkin M, M. X, Kalabukhov A, Winkler D (2016) Development of a 7- Channel High-Tc MEG System. *20th International conference on Biomagnetism 2016* WE-P048.

Pfurtscheller G, Stancak Jr A, Neuper C (1996) Post-movement beta synchronization. A correlate of an idling motor area? *Electroencephalography and Clinical Neurophysiology* 98:281-293.

Pizzella V, Della Penna S, Erné S, Granata C, Pasquarelli A, Torquati K, Rossi R, Russo M (2000) A 165-channel neuromagnetometer for multimodal brain imaging. In: Proceedings of the 12th International Conference on Biomagnetism, Helsinki.

Pool JL, Ransohoff J (1949) Autonomic effects on stimulating rostral portion of cingulate gyri in man. *Journal of Neurophysiology* 12:385-392.

Popov EV (2002) Geometric approach to chebyshev net generation along an arbitrary surface represented by nurbs. In: International Conference Graphicon.

Port RG, Anwar AR, Ku M, Carlson GC, Siegel SJ, Roberts TP (2015) Prospective MEG biomarkers in ASD: pre-clinical evidence and clinical promise of electrophysiological signatures. *The Yale Journal of Biology and Medicine* 88:25.

Romani GL, Williamson SJ, Kaufman L (1982) Biomagnetic instrumentation. *Review of Scientific Instruments* 53:1815-1845.

Sarvas J (1987) Basic mathematical and electromagnetic concepts of the biomagnetic inverse problem. *Physics in Medicine & Biology* 32:11.

Schneiderman JF (2014) Information content with low- vs. high-T(c) SQUID arrays in MEG recordings: the case for high-T(c) SQUID-based MEG. *J Neurosci Methods* 222:42-46.

Sherman MA, Lee S, Law R, Haegens S, Thorn CA, Hämäläinen MS, Moore CI, Jones SR (2016) Neural mechanisms of transient neocortical beta rhythms: converging evidence from humans, computational modeling, monkeys, and mice. *Proceedings of the National Academy of Sciences* 113:E4885-E4894.

Stefan H, Hummel C, Scheler G, Genow A, Druschky K, Tilz C, Kaltenhäuser M, Hopfengärtner R, Buchfelder M, Romstöck J (2003) Magnetic brain source imaging of focal epileptic activity: a synopsis of 455 cases. *Brain* 126:2396-2405.

Stoffers D, Bosboom J, Deijen J, Wolters EC, Stam CJ, Berendse HW (2008) Increased cortico-cortical functional connectivity in early-stage Parkinson's disease: an MEG study. *Neuroimage* 41:212-222.

Stufflebeam SM, Tanaka N, Ahlfors SP (2009) Clinical applications of magnetoencephalography. *Human Brain Mapping* 30:1813-1823.

Taulu S, Hari R (2009) Removal of magnetoencephalographic artifacts with temporal signal-space separation: demonstration with single-trial auditory-evoked responses. *Human Brain Mapping* 30:1524-1534.

Taulu S, Simola J (2006) Spatiotemporal signal space separation method for rejecting nearby interference in MEG measurements. *Physics in Medicine and Biology* 51:1759.

Timio M, Lippi G, Venanzi S, Gentili S, Quintaliani G, Verdura C, Monarca C, Saronio P, Timio F (1997) Blood pressure trend and cardiovascular events in nuns in a secluded order: a 30-year follow-up study. *Blood Pressure* 6:81-87.

Timio M, Verdecchia P, Venanzi S, Gentili S, Ronconi M, Francucci B, Montanari M, Bichisao E (1988) Age and blood pressure changes. A 20-year follow-up study in nuns in a secluded order. *Hypertension* 12:457-461.

Tomberg C, Desmedt JE, Ozaki I, Nguyen T, Chalklin V (1989) Mapping somatosensory evoked potentials to finger stimulation at intervals of 450 to 4000 msec and the issue of habituation when assessing early cognitive components. *Electroencephalography and Clinical Neurophysiology/Evoked Potentials Section* 74:347-358.

Troebinger L, López JD, Lutti A, Bestmann S, Barnes G (2014) Discrimination of cortical laminae using MEG. *Neuroimage* 102:885-893.

Van Veen BD, Van Drongelen W, Yuchtman M, Suzuki A (1997) Localization of brain electrical activity via linearly constrained minimum variance spatial filtering. *IEEE Transactions on Biomedical Engineering* 44:867-880.

Vogt BA, Derbyshire SW (2009) Visceral circuits and cingulate-mediated autonomic functions. *Cingulate Neurobiology and Disease* 219-236.

Wallin BG, Fagius J (1988) Peripheral sympathetic neural activity in conscious humans. *Annual review of Physiology* 50:565-576.

Wallin BG, Sundlöf G, Delius W (1975) The effect of carotid sinus nerve stimulation on muscle and skin nerve sympathetic activity in man. *Pflügers Archiv European Journal of Physiology* 358:101-110.

Zamrini E, Maestu F, Pekkonen E, Funke M, Makela J, Riley M, Bajo R, Sudre G, Fernandez A, Castellanos N (2011) Magnetoencephalography as a putative biomarker for Alzheimer's disease. *International Journal of Alzheimer's Disease* 2011.